

BIODEGRADABLE POLYMERIC NANOPARTICLES FOR CANCER
COMBINATION THERAPY

by

Joshua Heejae Choi

(Under the Direction of Shanta Dhar)

ABSTRACT

Many conventional therapies are used to treat various cancers. However, because of multiple problems that include low efficacy and safety issues, different strategies to treat cancer are necessary. One strategy is combination therapy. Combining drugs or other adjuvants has a synergistic effect in cancer treatments. Combination therapy permits multiple targeting through the same or different signaling pathways to overcome the limitations. Moreover, the use of nanotechnology in combination therapy permits even greater increases in efficacy. The U.S. Food and Drug Administration (FDA) has approved biodegradable polymers such as poly (D,L-lactide-*co*-glycolide) (PLGA) and poly (ethylene glycol) (PEG) that can be surface modified with targeting moiety for active targeting strategy. PLGA-*b*-PEG is used for formation of biodegradable polymeric nanoparticles for delivery of payloads. In this thesis, I report on several strategies of combination therapy using polymeric nanoparticles.

INDEX WORDS: cancer, combination therapy, biodegradable polymeric nanoparticles, immunotherapy, chemotherapy, inflammation

BIODEGRADABLE POLYMERIC NANOPARTICLES FOR CANCER
COMBINATION THERAPY

by

Joshua Heejae Choi

B.S., Iowa State University, 2009

A Thesis Submitted to the Graduate Faculty of the University of Georgia in Partial

Fulfillment of the Requirements for the Degree

MASTER OF SCIENCE

ATHENS, GEORGIA

2014

© 2014

Joshua Heejae Choi

All Rights Reserved

BIODEGRADABLE POLYMERIC NANOPARTICLES FOR CANCER
COMBINATION THERAPY

by

Joshua Heejae Choi

Major Professor: Shanta Dhar

Committee: Donald Harn
Robert Phillips

Electronic Version Approved:

Julie Coffield
Interim Dean of the Graduate School
The University of Georgia
December 2014

DEDICATION

For all of my family, Kyungil Choi, Hae Kyung Kang, Heeyoon Choi, Eunmi Shin, Lydia Heejoo Choi, and Sarah HyunJi Choi . Thank you for always supporting me. I could not make it through without their support in all aspects. I Love you all.

ACKNOWLEDGEMENTS

I would like to thank the University of Georgia for the funding and support throughout my graduate school. First, I would like to thank my principle advisor, Dr. Shanta Dhar. Her direction, care and all the support guided to be on a right track throughout my graduate career. Also, her enthusiasm towards science has inspired.

I would also like to thank to my advisory committee: Dr. Harn and Dr. Phillips for all the help. Their advices were a great help to complete my thesis. I also thank Dr. Smanla Tundup for assist me with many experiments from the beginning of my graduate year. Dhillon made nanoparticles for chapter 2 and Chinmaya made curcumin for chapter 3.

Finally, I thank to my research group member. Dr. Rakesh Pathak and Dr. Sean Marrache have supported me in every aspect in research group. Without their help and care, I would have hard time working. I also enjoyed working with all the undergraduate researchers in our lab. I also thank to Dr. Nagesh Kolishetti. His advices were very supportive.

TABLE OF CONTENTS

	Page
DEDICATIONS.....	iv
ACKNOWLEDGEMENTS.....	v
LIST OF TABLES.....	viii
LIST OF FIGURES.....	ix
CHAPTER	
1 INTRODUCTION AND LITERATURE REVIEW.....	1
Cancer.....	1
Combination Therapy.....	1
Nanotechnology and Nanomedicine.....	2
Biodegradable Polymeric NPs.....	4
PEGylated Polymeric NPs.....	5
Passive and Active Targeting.....	6
NP Characterization to Overcome Biological Barrier.....	8
Objective and Outline of the Thesis.....	11
References.....	12
2 IMMUNE STIMULATING PHOTOACTIVE HYBRID NANOPARTICLES FOR METASTATIC BREAST CANCER.....	24
Abstract.....	25

Introduction.....	26
Experimental.....	29
Results and Discussions.....	33
Conclusions.....	40
References.....	42
3 CHEMO-ANTI-INFLAMMATORY THERAPY FOR CANCER.....	45
Introduction.....	45
Experimental.....	47
Results and Discussions.....	56
Conclusions.....	79
References.....	80
4 Conclusion and Outlook.....	84
Conclusion.....	84
Future Work.....	85
Final Remarks.....	85

LIST OF TABLES

	Page
Table 1.1: Polymers for Biodegradable Polymeric NPs	4
Table 2.1: Comparison of molecular weights of PLGA-COOH and PLGA- <i>b</i> -PEG-NH ₂ as determined from gel permeation chromatographic (GPC)	35
Table 2.2: Loading efficiencies of ZnPc at various weight percentage with respect to the polymer.	36
Table 2.3: Stability of CpG-ODN-Au-ZnPc-Poly-NPs by DLS measurements in nanopure water	39
Table 3.1: Comparison of IC ₅₀ values of cisplatin, an equimolar mixture of cisplatin and aspirin, and Platin-A in different PCa cells.	57
Table 3.2: Comparison of molecular weights of PLGA-COOH, PLGA- <i>b</i> -PEG-NH ₂ , and PLGA- <i>b</i> -PEG-TPP as determined from gel permeation chromatographic (GPC) with THF.	74
Table 3.3: Comparison of IC ₅₀ values of Platin-C NPs, free form of Platin-C, cisplatin, curcumin and an equimolar mixture of cisplatin and curcumin in A2780/CP70(top left), MCF-7(top right), and DU145(bottom) cell lines.	79

LIST OF FIGURES

	Page
Figure 1.1: Various nanotechnology-based delivery vehicles	3
Figure 1.2: Schematic representation of passive and active targeting	8
Figure 1.3: Biodistribution and clearance of nanoparticles	10
Figure 2.1: Phagocytosis of tumor antigens by DCs after PDT.....	27
Figure 2.2: Schematic diagram of the NP platform for combination therapy of metastatic breast cancer.	28
Figure 2.3 ^1H and ^{13}C NMR of PLGA- <i>b</i> -PEG-NH ₂	34
Figure 2.4: Photographs of NP suspensions with no visible aggregation.....	37
Figure 2.5: Hydrodynamic diameter and zeta potential of the NPs by DLS measurements.....	37
Figure 2.6: Characterization of hybrid NPs by UV-Vis spectroscopy.....	38
Figure 2.7: TEM images of ZnPc-Poly-NPs, Au-ZnPc-Poly-NPs, and CpG-ODN-Au-ZnPc-Poly-NPs..	38
Figure 2.8: Cytotoxicity profiles in 4T1 cells in the dark (left) and after 5 min exposure with a 660 nm Laser (right).	40
Figure 3.1: Cytotoxic profiles of Platin-A, cisplatin, and an equimolar mixture of cisplatin and aspirin in PCa cell lines.	57
Figure 3.2: Inhibition of ovine COX-1 and COX-2 by Platin-A.....	58
Figure 3.3: Schematic diagram of synthesis of Pt(IV)(curcumin) ₂	59

Figure 3.4: ^1H NMR, ^{13}C NMR of $\text{Pt(IV)(curcumin)}_2$ in DMSO-d_6 .	60
Figure 3.5: Full and extended spectrum of 2D NMR of $\text{Pt(IV)(curcumin)}_2$ in DMSO-d_6 .	61-62
Figure 3.6: Full spectrum (top) and positive spectrum (bottom) ^{195}Pt NMR of $\text{Pt(IV)(curcumin)}_2$ in DMSO-d_6 .	63
Figure 3.7: Positive ion ESI-HRMS spectrum of $\text{Pt(IV)(curcumin)}_2$.	64
Figure 3.8: Observed (top) and calculated (bottom) isotopic peak pattern analysis of Positive ion ESI-HRMS spectrum of $\text{Pt(IV)(curcumin)}_2$.	64-65
Figure 3.9: HPLC analysis of $\text{Pt(IV)(curcumin)}_2$ and curcumin.	65
Figure 3.10: Schematic diagram of synthesis of Platin-C.	66
Figure 3.11: ^1H NMR and ^{13}C NMR of Platin-C in DMSO-d_6 .	67
Figure 3.12: Full spectrum (top) and positive spectrum (bottom) ^{195}Pt NMR of Platin-C in DMSO-d_6 .	68
Figure 3.13: Positive ion ESI-HRMS spectrum of Platin-C.	69
Figure 3.14: Isotopic peak pattern analysis of Positive ion ESI-HRMS spectrum of Platin-C.	69-70
Figure 3.15: HPLC analysis of Platin-C and curcumin.	70
Figure 3.16: Schematic diagram of synthesis of non targeted and targeted Polymers and Formation of NPs.	72
Figure 3.17: ^1H and ^{13}C NMR of PLGA-PEG-TPP (Targeted polymer).	73
Figure 3.18: GPC of different Polymers.	74
Figure 3.19: Diameter and Zeta Potential of Different weight percentage of Platin-C NPs.	76

Figure 3.20: % Loading Efficiency and % Encapsulation Efficiency of NPs	76
Figure 3.21: TEM of 20% NT (left) and T (right) NPs	77
Figure 3.22: Cytotoxic profiles of Platin-C NPs, free form of Platin-C, cisplatin, curcumin and an equimolar mixture of cisplatin and curcumin in A2780/CP70(top left), MCF-7(top right), and DU145(bottom) cell lines...	78

CHAPTER 1

INTRODUCTION AND LITERATURE REVIEW

Cancer

Cancer is a fatal disease characterized by the uncontrolled growth and spread of abnormal cells^{1,2}. It can be caused by external factors such as tobacco, infectious organisms, chemicals, diets, and radiation as well as internal factors such as inherited mutations, immune conditions, and multiple mutations³⁻¹⁵. These factors can act separately or simultaneously to initiate or promote the development of cancer¹⁶.

Cancer is a major public health problem not only in United States but also in many other parts of the world. It is the second most common cause of death in United States; one in 4 deaths are caused by cancer¹⁶. Moreover, approximately 13.7 million Americans have a history of cancer as either cancer-free survivors or as patients undergoing treatment¹⁶. However, the mortality rate from cancer has decreased continuously for two decades because of a better understanding of tumor biology, improved diagnostics, and new treatments^{1, 17, 18}.

Combination Therapy

Conventional therapies to treat cancer are chemotherapy, surgery, radiation, immune therapy, and photodynamic therapy^{1, 2, 19-25}. However, these therapies have numerous limitations such as toxicity, non-selective killing of live cells along with cancer cells, damage to nearby tissues, and operative failure with the latter especially associated with surgery^{22, 26-28}. Also,

chemotherapy often has side effects and some types of cancer develop resistance towards particular chemotherapeutic drugs^{20, 29-32}.

First line therapy for cancer is chemotherapy³²⁻³⁶. Recent research to discover new drugs has focused on development of drugs on individual targets³⁷⁻³⁹. However this research has encountered some problems such as low therapeutic efficacy, safety issues, and resistance profiles. Progress in understanding molecular mechanisms and the cell signaling pathways of current drugs provide clues to synergistic targets for more effective treatments²⁸. Furthermore, this progress offers synergistic and potential effects of combination therapy that can deliver the best outcomes from treatment. Combination therapy confers advantages over single drug therapy such as multiple targeting with the same or different signaling pathways, increased therapeutic efficacy, and lessened drug resistance^{32, 36, 40-42}. One of the combination therapies can be chemo-anti-inflammatory therapy. Advanced cancer is highly related with inflammation. Controlling inflammation and eradicating the primary tumor simultaneously can delay the progression of tumor effectively⁴³. Another approach can be photoimmunotherapy. Cancer therapies are mostly known to be immunosuppressive^{2, 19}. However, photodynamic therapy, use of photosensitizer, a drug with light irradiation to kill cancer, is an immune activating^{19, 44} therapy which can exhibit synergistic effect when it combines with immunotherapy^{45, 46}. The biggest advantages of this is that it not only treats primary cancer but also metastatic cancer⁴⁵.

Nanotechnology and Nanomedicine

Nanomedicine is the application of nanotechnology to medicine⁴⁷. The use of nanotechnology-based drug delivery allows monitoring the distribution, release, response, and efficacy of an on-demand controlled drug release that can in turn help overcome both over and under dosing, a common dosage flaw associated with conventional drug treatments^{48, 49}. In other

word, nanomedicine is a clinical practice that diagnose, prevent, and treat numerous disease with the use of nanotechnologies. According to the National Nanotechnology Initiative (NNI), nanotechnology is defined as research and development carried out at the atomic to macro molecular levels on the scale of 1 – 100 nm range⁴⁸. However, the size limitation is not critical. Instead, the most important properties in the transition of nanotechnology to nanomedicine are improved solubility, physiological availability, and lowered drug dosages and toxicity, all of which may be achieved in a size range greater than 100 nm. Nanomaterials are widely spread, but yet, some of them require the way to use for clinical practices. Metal based nanoparticles (NPs), polymeric NPs, micelles, liposome, and dendrimers are examples of nanomaterials (Figure 1.1.)⁵⁰.

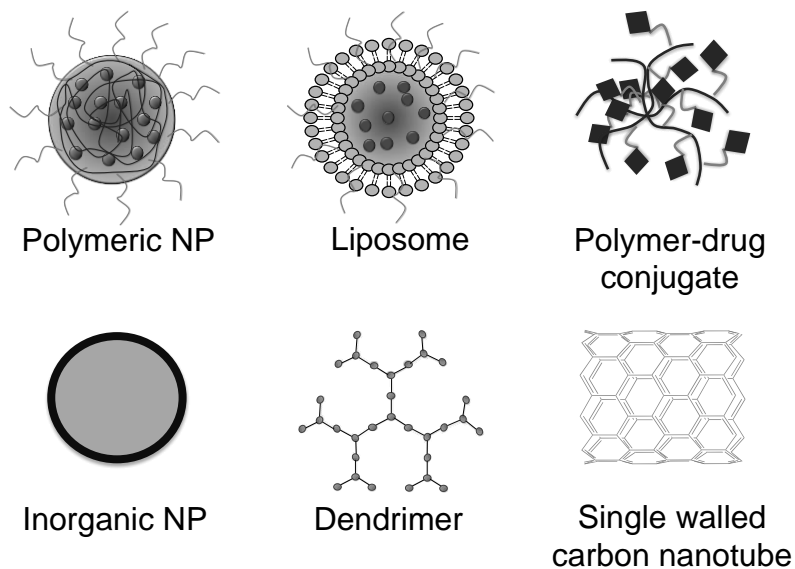


Figure 1.1. Various nanotechnology-based delivery vehicles⁵¹.

Biodegradable Polymeric NPs

In 1964, Folkman and Long invented the concept of therapeutic loading of an implantable, controlled-release polymeric vehicle⁵². The remarkable work by Langer and Folkman in 1976 led to the launch of “controlled release drug delivery”⁵³. Since then, a number of polymeric materials and devices for therapeutic delivery have enriched this area of research⁵⁴.⁵⁵. Rapid advancement in recent years has brought controlled drug delivery systems that include polymeric NPs based on biodegradable and biocompatible polymers. These polymers degrade spontaneously in a predetermined and controlled manner into bio-friendly end products that can be eliminated from the body^{48, 56-72}. The biocompatible and biodegradable polymers that are used to construct NPs can be natural or synthetic (Table 1.1.).

Table 1.1. Polymers for Biodegradable Polymeric NPs⁵¹.

Natural Polymers	Synthetic Polymers
Polysaccharides: Hyaluronate, Dextran, Chitosan, Alginate, Agarose etc. Protein-based polymers: Fibrin, Collagen, Ferritin	Poly (glycolic acid) (PGA), Poly (lactic acid) (PLA), and copolymer poly(lactide- <i>co</i> -glycolides) (PLGA), polycaprolactone (PCL), Poly (ethylene glycol) (PEG) and its derivatives and copolymers, Polyamides, Polyamides, Poly (vinyl alcohol) PVA, Polypeptides

Poly(lactic acid) (PLA), poly(glycolic acid) (PGA), their copolymer poly(D,L-lactide-*co*-glycolide) (PLGA) are biodegradable and biocompatible polymers, approved by the Food and

Drug Administration (FDA), that are commonly used for controlled and sustained release in medical applications. Polymeric nanocarriers can be constructed by conjugating payloads to soluble macromolecules, and polymeric NPs can be synthesized by co-polymer self-assembly. In a self-assembled material, the polymeric NP matrix can be loaded with a variety of payloads⁷³. Polymeric backbone can be cleaved chemically and enzymatically. Cleavage occurs by catalysts from physiological environment or ones embedded within the polymer or by hydrolytic degradation. Cleavage causes a drop of polymer molecular weight that leads to the erosion of the biomaterial. There are two types of erosion, which are homogeneous bulk disintegration or heterogeneous surface erosion. Diffusion of the drug and the eroding nature of the matrix regulates the release of payloads. Erosion can be homogenous bulk disintegration or heterogeneous surface erosion. Bulk erosion takes place in the entire polymeric matrix where surface erosion occurs on surface of the polymeric matrix. Bulk erosion is caused by rate of water penetration so that release of drug depends on drug diffusion. However, because the degradation rate of the surface that is faster than the rate of water penetration, drug release depends on both drug diffusion and matrix degradation. Biodegradable polymers make abundant use of both types of degradation processes. Conversely, conjugation of payloads to the polymer backbone allows for predetermined drug loading with control over drug release profiles and creates opportunities to load multiple therapeutics with spatio temporal release profiles for combination therapy⁶⁸.

PEGylated Polymeric NPs

Polymeric NPs can be further coated with a hydrophilic polymer to inhibit opsonization and to enhance water solubility. A well-accepted practice for control of the stability and immunogenicity of polymeric NPs includes incorporation of polyethylene glycol (PEG) by adsorption or covalent attachment⁴⁷, which is a biocompatible non-ionic hydrophilic polymer

with stealth behavior⁷⁴ and that the FDA has approved for clinical use. NP formulations with increased stability are usually obtained by incorporation of PEG, which provides suitable steric stabilization and thereby reduces the tendency to aggregate. The unique properties of PEG can influence the pharmacokinetic (PK) profiles of therapeutics as well as the polymeric NP carrier. The presence of PEG in polymeric NPs results in increased blood circulation times⁵⁸. Most of the polymer-based delivery systems that are in the market contain PEG functionalized products that are called PEGylated.

Passive and Active Targeting

The blood vessels in most solid tumors differ uniquely from normal blood vessels in several ways: (i) active angiogenesis and high vascular density; (ii) extensive extravasation by vascular mediators; (iii) defective vascular architecture; and (iv) impaired lymphatic clearance of macromolecules and lipids from interstitial tissue⁷⁵. These characteristics enhance the permeability to macromolecule and NPs. Moreover, the dysfunction of the lymphatic drainage system contributes to their retention for longer periods. The concentration of polymeric NPs and macromolecules in tumor tissues can be up to 100x higher than in normal tissues^{76,77}. This tumor-specific deposition because of the unique characteristics of tumor vessels is known as the enhanced permeability and retention (EPR) effect. It is a passive targeting approach that most NPs and macromolecules use to accumulate preferentially. Experiments using different sizes of liposomes suggest that the pore cutoff size for extravasation into tumor is 400-600 nm⁷⁸; however, in general, particles with diameters of less than 200 nm are more effective for extravasation⁷⁸⁻⁸¹.

However, this passive targeting method has some limitations. Depending on the drug involved, these limitations differ from diffusion efficiencies such as low vascular densities that

are common in certain tumors, such as in pancreatic and prostate cancer, lessen the EPR effect⁸² and the irregular permeability of vessels within tumors. These limitations give the approach a random nature that complicates control of a process that can induce multiple-drug resistance (MRD). Because of the resistance of cancer cells towards drugs, therapeutic efficiency inevitably declines⁸³⁻⁸⁵.

To overcome these limitations, surface modification of particles is necessary. This permits active targeting so that particles are delivered to more specific sites with minimal undesired effects. By conjugating targeting agents to the particle surface that can only be recognized and bind to specific receptors that are uniquely expressed in certain cells, more deposition occurs on the target cells.

Targeting molecules can be classified as proteins (monoclonal antibodies), nucleic acids (aptamers), and receptor ligands (peptides, vitamins, and carbohydrates). Monoclonal antibodies (mAb) were introduced in 1981 by Milstein as the first molecules for targeting cancer⁸⁶. Over the decades since, antibody-based targeting molecules have been demonstrated clinically⁸⁷. Antibodies can be used in their native states or as fragments. However, the native state of an antibody has two binding sites: the presence of two sites yields a higher binding propensity than occurs with fragments. Another form of targeting molecules, aptamers, has single-stranded DNA or RNA that can bind to a target with high affinity and specificity⁸⁸. Aptamers are selected in vitro via a process called systemic evolution of ligands by exponential enrichment (SELEX), from a large number of oligonucleotides^{89,90}. Other targeting agents such as peptides attract a lot of attention because of their small size, lower immunogenicity, higher stability, and ease of manufacture. Similarly, high-affinity vitamins and folic acid (folate) get attention because folate

receptors are usually overexpressed in a tumor cells⁹¹. Figure 1.2. shows a schematic representation of passive and active targeting particles¹⁷.

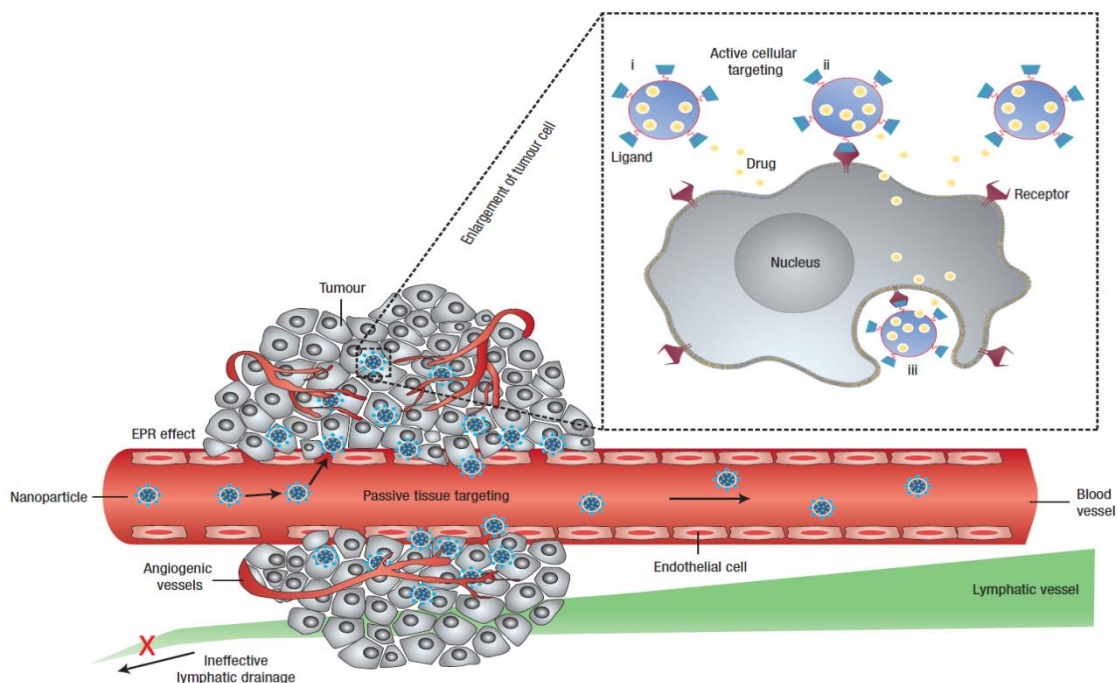


Figure 1.2. Schematic representation of passive and active targeting¹⁷.

NP characterization to overcome biological barrier

The human body has numerous biological barriers, such as the immune system, to protect from foreign substances. Particles must overcome these barriers to reach the target and to perform their functions. One biological barrier is the reticuloendothelial system (RES). RES is also called the macrophage system or mononuclear phagocyte system which is a defense mechanism of class of cells, which identify and filter out dead, toxic, or foreign particles in the blood and tissues⁹². Particles swept up by macrophages end up accumulating in the liver and spleen⁹³. Another barrier is clearance through excretion. It can be excreted depends on size, which determines whether it will accumulate more in the kidneys than in the targeted site.

However, NPs are suited to overcome these barriers because of their unique size and amenability to surface modification. Because of physiological parameters such as hepatic filtration, tissue extravasation, and kidney excretion, particle size is a major factor that can improve therapeutic efficiency. Protein adsorption and blood clearance kinetics were studied on different size pegylated PHDCA nanoparticles⁹⁴. The results showed that small nanoparticles (~80 nm) adsorb less than a larger size (>100 nm) and blood clearance was twice as slow as with larger nanoparticles. Nevertheless, less than 10 nm NPs are excreted via the kidneys. Not only size but also the charge and surface functionality are important. Polystyrene microparticles with a primary amine underwent more phagocytosis than microparticles with surface of sulfate, hydroxyl, and carboxyl groups. This demonstrates that positively charged particles are taken up more than neutral or negatively charged particles⁵⁸. According to the experiment, smaller pegylated particles have a higher PEG density to increase the period of blood circulation period and pegylated particles with <100 nm with neutral or negative charge lower protein adsorption, eventually reducing hepatic filtration. Although a smaller particle size is preferred, particles less than 10 nm will be cleared through kidney excretion. Figure 1.3. shows the biodistribution and clearance of nanoparticles⁵⁸.

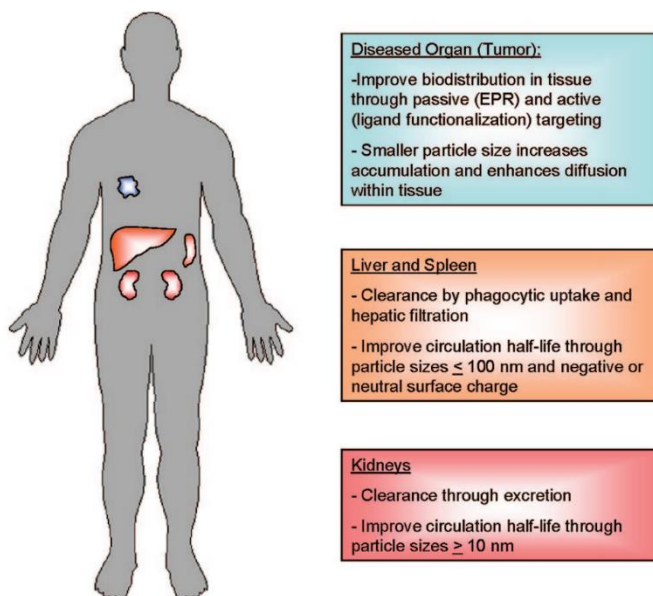


Figure. 1.3. Biodistribution and clearance of nanoparticles⁵⁸.

Objective and Outline of the Thesis

The objective of this thesis is to develop advanced therapeutic modalities for cancer treatment that are based on combination therapy with nanotechnology; accomplishing this involves the following: (i) design of a combination therapy method, small molecules, and biodegradable NPs and (ii) evaluation of the potency of these therapeutic in different types of cancer. The rest of this thesis is organized into three chapters.

Chapter 2 investigates the combination of photodynamic therapy and immunotherapy. Photosensitizer, zinc phthalocyanine (ZnPc), encapsulated with biodegradable polymeric NPs and CpG-ODN, immunostimulant, was conjugated to gold NPs covalently that are incorporated to the surface of polymeric NPs noncovalently. Phototoxicity and the immune response were determined by using the (3-(4,5-dimethylthiazol-2-yl)-2,5-diphenyltetrazolium bromide (MTT) assay and enzyme-linked immunosorbent assay (ELISA) respectively. This chapter was published in *Integrative Biology*, 2013, 5, 215-223.

Chapter 3 describes the development of novel, and new cisplatin prodrug for chemo-anti-inflammatory therapy. Anti-inflammatory drugs, aspirin or curcumin, were conjugated to cisplatin via acid anhydride reaction. They were encapsulated with NP that functionalized with targeting moiety as delivery cargo to test the cytotoxicity on prostate, breast, and cisplatin-resistant ovarian cancer cells *in vitro*. Moreover, anti-inflammatory effects were tested to confirm the combination effect.

Finally, Chapter 4 summarizes each project discussed and discusses impact on future studies.

References

1. Brannon-Peppas, L.; Blanchette, J. O., Nanoparticle and targeted systems for cancer therapy. *Adv. Drug Delivery Rev.* **2012**, *64*, 206-212.
2. Zitvogel, L.; Apetoh, L.; Ghiringhelli, F.; Kroemer, G., Immunological aspects of cancer chemotherapy. *Nat. Rev. Immunol.* **2008**, *8* (1), 59-73.
3. Denissenko, M. F.; Pao, A.; Tang, M.-s.; Pfeifer, G. P., Preferential formation of benzo[a] pyrene adducts at lung cancer mutational hotspots in P53. *Science* **1996**, *274* (5286), 430-432.
4. Anto, R. J.; Mukhopadhyay, A.; Shishodia, S.; Gairola, C. G.; Aggarwal, B. B., Cigarette smoke condensate activates nuclear transcription factor- κ B through phosphorylation and degradation of I κ B α : correlation with induction of cyclooxygenase-2. *Carcinogenesis* **2002**, *23* (9), 1511-1518.
5. Tuyns, A., Epidemiology of alcohol and cancer. *Cancer Res.* **1979**, *39* (7 Part 2), 2840-2843.
6. Seitz, H. K.; Stickel, F.; Homann, N., Pathogenetic mechanisms of upper aerodigestive tract cancer in alcoholics. *Int. J. Cancer* **2004**, *108* (4), 483-487.
7. Doll, R.; Peto, R., The causes of cancer: quantitative estimates of avoidable risks of cancer in the United States today. *J. Natl. Cancer I.* **1981**, *66* (6), 1192-1308.
8. Williams, R. R.; Horm, J. W., Association of cancer sites with tobacco and alcohol consumption and socioeconomic status of patients: interview study from the Third National Cancer Survey. *J. Natl. Cancer I.* **1977**, *58* (3), 525-547.
9. Pisani, P.; Parkin, D. M.; Munoz, N.; Ferlay, J., Cancer and infection: estimates of the attributable fraction in 1990. *Cancer Epid. Biomar.* **1997**, *6* (6), 387-400.

10. Parkin, D. M., The global health burden of infection-associated cancers in the year 2002. *Int. J. Cancer* **2006**, *118* (12), 3030-3044.
11. Willett, W. C., Diet and cancer. *The Oncologist* **2000**, *5* (5), 393-404.
12. Belpomme, D.; Irigaray, P.; Hardell, L.; Clapp, R.; Montagnier, L.; Epstein, S.; Saso, A. J., The multitude and diversity of environmental carcinogens. *Environ. Res.* **2007**, *105* (3), 414-429.
13. Lichtenstein, P.; Holm, N. V.; Verkasalo, P. K.; Iliadou, A.; Kaprio, J.; Koskenvuo, M.; Pukkala, E.; Skytthe, A.; Hemminki, K., Environmental and heritable factors in the causation of cancer—analyses of cohorts of twins from Sweden, Denmark, and Finland. *N. Engl. J. Med.* **2000**, *343* (2), 78-85.
14. Loeb, K. R.; Loeb, L. A., Significance of multiple mutations in cancer. *Carcinogenesis* **2000**, *21* (3), 379-385.
15. Hahn, W. C.; Weinberg, R. A., Modelling the molecular circuitry of cancer. *Nat. Rev. Cancer* **2002**, *2* (5), 331-341.
16. Siegel, R.; Ma, J.; Zou, Z.; Jemal, A., Cancer statistics, 2014. *CA Cancer J. Clin.* **2014**, *64* (1), 9-29.
17. Peer, D.; Karp, J. M.; Hong, S.; Farokhzad, O. C.; Margalit, R.; Langer, R., Nanocarriers as an emerging platform for cancer therapy. *Nat. Nanotechnol.* **2007**, *2* (12), 751-760.
18. Kesari, S. In Understanding glioblastoma tumor biology: the potential to improve current diagnosis and treatments, *Semin. Oncol.*, Elsevier: 2011; pp S2-S10.
19. Castano, A. P.; Mroz, P.; Hamblin, M. R., Photodynamic therapy and anti-tumour immunity. *Nat. Rev. Cancer* **2006**, *6* (7), 535-545.

20. Gee, J.; Howell, A.; Gullick, W.; Benz, C.; Sutherland, R.; Santen, R.; Martin, L.; Ciardiello, F.; Miller, W.; Dowsett, M., Consensus statement. *Endocr.-Relat Cancer* **2005**, *12* (Supplement 1), S1-S7.
21. Chabner, B. A.; Roberts, T. G., Chemotherapy and the war on cancer. *Nat. Rev. Cancer* **2005**, *5* (1), 65-72.
22. Wood, A. J.; Shapiro, C. L.; Recht, A., Side effects of adjuvant treatment of breast cancer. *N. Engl. J. Med.* **2001**, *344* (26), 1997-2008.
23. Kelsen, D. P.; Ginsberg, R.; Pajak, T. F.; Sheahan, D. G.; Gunderson, L.; Mortimer, J.; Estes, N.; Haller, D. G.; Ajani, J.; Kocha, W., Chemotherapy followed by surgery compared with surgery alone for localized esophageal cancer. *N. Engl. J. Med.* **1998**, *339* (27), 1979-1984.
24. Turcotte, S.; Rosenberg, S. A., Immunotherapy of Metastatic Solid Cancers. *Adv. Surg.* **2011**, *45*, 341.
25. Dolmans, D. E.; Fukumura, D.; Jain, R. K., Photodynamic therapy for cancer. *Nat. Rev. Cancer* **2003**, *3* (5), 380-387.
26. Kelland, L., The resurgence of platinum-based cancer chemotherapy. *Nat. Rev. Cancer* **2007**, *7* (8), 573-584.
27. Simmonds, P.; Primrose, J.; Colquitt, J.; Garden, O.; Poston, G.; Rees, M., Surgical resection of hepatic metastases from colorectal cancer: a systematic review of published studies. *Br. J. Cancer* **2006**, *94* (7), 982-999.
28. Jia, J.; Zhu, F.; Ma, X.; Cao, Z. W.; Li, Y. X.; Chen, Y. Z., Mechanisms of drug combinations: interaction and network perspectives. *Nat. Rev. Drug Discov.* **2009**, *8* (2), 111-128.

29. Elmore, L. W.; Di, X.; Dumur, C.; Holt, S. E.; Gewirtz, D. A., Evasion of a single-step, chemotherapy-induced senescence in breast cancer cells: implications for treatment response. *Clin. Cancer Res.* **2005**, *11* (7), 2637-2643.
30. Komarova, E. A.; Chernov, M. V.; Franks, R.; Wang, K.; Armin, G.; Zelnick, C. R.; Chin, D. M.; Bacus, S. S.; Stark, G. R.; Gudkov, A. V., Transgenic mice with p53-responsive lacZ: p53 activity varies dramatically during normal development and determines radiation and drug sensitivity in vivo. *The EMBO journal* **1997**, *16* (6), 1391-1400.
31. Siddik, Z. H., Cisplatin: mode of cytotoxic action and molecular basis of resistance. *Oncogene* **2003**, *22* (47), 7265-7279.
32. Bello, L.; Carrabba, G.; Giussani, C.; Lucini, V.; Cerutti, F.; Scaglione, F.; Landré, J.; Pluderi, M.; Tomei, G.; Villani, R., Low-dose chemotherapy combined with an antiangiogenic drug reduces human glioma growth in vivo. *Cancer Res.* **2001**, *61* (20), 7501-7506.
33. Perry, M. C., *The chemotherapy source book*. Lippincott Williams & Wilkins: 2008.
34. Tanabe, M.; Ito, Y.; Tokudome, N.; Sugihara, T.; Miura, H.; Takahashi, S.; Seto, Y.; Iwase, T.; Hatake, K., Possible use of combination chemotherapy with mitomycin C and methotrexate for metastatic breast cancer pretreated with anthracycline and taxanes. *Breast cancer* **2009**, *16* (4), 301-306.
35. Berhoune, M.; Banu, E.; Scotte, F.; Prognon, P.; Oudard, S.; Bonan, B., Therapeutic strategy for treatment of metastatic non-small cell lung cancer. *Ann. Pharmacother.* **2008**, *42* (11), 1640-1652.

36. Douillard, J.; Cunningham, D.; Roth, A.; Navarro, M.; James, R.; Karasek, P.; Jandik, P.; Iveson, T.; Carmichael, J.; Alakl, M., Irinotecan combined with fluorouracil compared with fluorouracil alone as first-line treatment for metastatic colorectal cancer: a multicentre randomised trial. *The Lancet* **2000**, *355* (9209), 1041-1047.
37. Drews, J., Drug discovery: a historical perspective. *Science* **2000**, *287* (5460), 1960-1964.
38. Imming, P.; Sinning, C.; Meyer, A., Drugs, their targets and the nature and number of drug targets. *Nat. Rev. Drug Discov.* **2006**, *5* (10), 821-834.
39. Zheng, C.; Han, L.; Yap, C.; Ji, Z.; Cao, Z.; Chen, Y., Therapeutic targets: progress of their exploration and investigation of their characteristics. *Pharmacol. Rev.* **2006**, *58* (2), 259-279.
40. Broxterman, H. J.; Georgopapadakou, N. H., Anticancer therapeutics: "Addictive" targets, multi-targeted drugs, new drug combinations. *Drug Resist. Update* **2005**, *8* (4), 183-197.
41. Dhar, S.; Lippard, S. J., Mitaplatin, a potent fusion of cisplatin and the orphan drug dichloroacetate. *Proc. Natl. Acad. Sci.* **2009**, *106* (52), 22199-22204.
42. Azrak, R. G.; Frank, C. L.; Ling, X.; Slocum, H. K.; Li, F.; Foster, B. A.; Rustum, Y. M., The mechanism of methylselenocysteine and docetaxel synergistic activity in prostate cancer cells. *Mol. Cancer Ther.* **2006**, *5* (10), 2540-2548.
43. Duffy, C.; Elliott, C.; O'Connor, R.; Heenan, M.; Coyle, S.; Cleary, I.; Kavanagh, K.; Verhaegen, S.; O'Loughlin, C.; NicAmhlaibh, R., Enhancement of chemotherapeutic drug toxicity to human tumour cells *in vitro* by a subset of non-steroidal anti-inflammatory drugs (NSAIDs). *Eur. J. Cancer* **1998**, *34* (8), 1250-1259.
44. Gollnick, S. O.; Owczarczak, B.; Maier, P., Photodynamic therapy and anti-tumor immunity. *Laser. Surg. Med.* **2006**, *38* (5), 509-515.

45. Qiang, Y. G.; Yow, C.; Huang, Z., Combination of photodynamic therapy and immunomodulation: current status and future trends. *Med. Res. Rev.* **2008**, *28* (4), 632-644.
46. Denis, T. G. S.; Aziz, K.; Waheed, A. A.; Huang, Y.-Y.; Sharma, S. K.; Mroz, P.; Hamblin, M. R., Combination approaches to potentiate immune response after photodynamic therapy for cancer. *Photochem. Photobiol. Sci.* **2011**, *10* (5), 792-801.
47. Freitas Jr, R. A., What is nanomedicine? *Nanomed-Nanotechnol* **2005**, *1* (1), 2-9.
48. Farokhzad, O. C.; Langer, R., Impact of nanotechnology on drug delivery. *ACS Nano* **2009**, *3* (1), 16-20.
49. Shi, J.; Votruba, A. R.; Farokhzad, O. C.; Langer, R., Nanotechnology in drug delivery and tissue engineering: from discovery to applications. *Nano Lett.* **2010**, *10* (9), 3223-3230.
50. Kamaly, N.; Xiao, Z.; Valencia, P. M.; Radovic-Moreno, A. F.; Farokhzad, O. C., Targeted polymeric therapeutic nanoparticles: design, development and clinical translation. *Chem. Soc. Rev.* **2012**, *41* (7), 2971-3010.
51. Marrache, S.; Kumar Pathak, R.; L Darley, K.; H Choi, J.; Zaver, D.; Kolishetti, N.; Dhar, S., Nanocarriers for tracking and treating diseases. *Curr. Med. Chem.* **2013**, *20* (28), 3500-3514.
52. Folkman, J.; Long, D. M., The use of silicone rubber as a carrier for prolonged drug therapy. *J. Surg. Res.* **1964**, *4* (3), 139-142.
53. Langer, R.; Folkman, J., Polymers for the sustained release of proteins and other macromolecules. *Nature* **1976**, *263* (5580), 797-800.
54. Langer, R., Drug delivery. Drugs on target. *Science* **2001**, *293* (5527), 58-9.

55. Richards Grayson, A. C.; Choi, I. S.; Tyler, B. M.; Wang, P. P.; Brem, H.; Cima, M. J.; Langer, R., Multi-pulse drug delivery from a resorbable polymeric microchip device. *Nat. Mater.* **2003**, *2* (11), 767-772.
56. Marrache, S.; Dhar, S., Engineering of blended nanoparticle platform for delivery of mitochondria-acting therapeutics. *Proc. Natl. Acad. Sci. USA* **2012**, *109* (40), 16288-16293.
57. Alexis, F.; Basto, P.; Levy-Nissenbaum, E.; Radovic-Moreno, A. F.; Zhang, L.; Pridgen, E.; Wang, A. Z.; Marein, S. L.; Westerhof, K.; Molnar, L. K.; Farokhzad, O. C., HER-2-targeted nanoparticle-affibody bioconjugates for cancer therapy. *ChemMedChem* **2008**, *3*, 1839-1843.
58. Alexis, F.; Pridgen, E.; Molnar, L. K.; Farokhzad, O. C., Factors affecting the clearance and biodistribution of polymeric nanoparticles. *Mol Pharm* **2008**, *5* (4), 505-515.
59. Bagalkot, V.; Zhang, L.; Levy-Nissenbaum, E.; Jon, S.; Kantoff, P. W.; Langer, R.; Farokhzad, O. C., Quantum dot-aptamer conjugates for synchronous cancer imaging, therapy, and sensing of drug delivery based on bi-fluorescence resonance energy transfer. *Nano Lett.* **2007**, *7* (10), 3065-3070.
60. Chan, J. M.; Zhang, L.; Yuet, K. P.; Liao, G.; Rhee, J. W.; Langer, R.; Farokhzad, O. C., PLGA-lecithin-PEG core-shell nanoparticles for controlled drug delivery. *Biomaterials* **2009**, *30* (8), 1627-34.
61. Cheng, J.; Teply, B. A.; Sherifi, I.; Sung, J.; Luther, G.; Gu, F. X.; Levy-Nissenbaum, E.; Radovic-Moreno, A. F.; Langer, R.; Farokhzad, O. C., Formulation of functionalized PLGA-PEG nanoparticles for in vivo targeted drug delivery. *Biomaterials* **2007**, *28* (5), 869-876.

62. Cheng, J.; Teply, B. A.; Sherifi, I.; Sung, J.; Luther, G.; Gu, F. X.; Levy-Nissenbaum, E.; Radovic-Moreno, A. F.; Langer, R.; Farokhzad, O. C., Formulation of functionalized PLGA-PEG nanoparticles for in vivo targeted drug delivery. *Biomaterials* **2008**, *28*, 868-876.
63. Dhar, S.; Gu, F. X.; Langer, R.; Farokhzad, O. C.; Lippard, S. J., Targeted delivery of cisplatin to prostate cancer cells by aptamer functionalized Pt(IV) prodrug-PLGA-PEG nanoparticles. *Proc. Natl. Acad. Sci. USA* **2008**, *105* (45), 17356-17361.
64. Dhar, S.; Kolishetti, N.; Lippard, S. J.; Farokhzad, O. C., Targeted delivery of a cisplatin prodrug for safer and more effective prostate cancer therapy in vivo. *Proc. Natl. Acad. Sci. USA* **2011**, *108* (5), 1850-1855.
65. Farokhzad, O. C.; Jon, S. Y.; Khadelmhosseini, A.; Tran, T. N. T.; LaVan, D. A.; Langer, R., Nanoparticle-aptamer bioconjugates: A new approach for targeting prostate cancer cells. *Cancer Res.* **2004**, *64* (21), 7668-7672.
66. Gu, F.; Zhang, L.; Teply, B. A.; Mann, N.; Wang, A.; Radovic-Moreno, A. F.; Langer, R.; Farokhzad, O. C., Precise engineering of targeted nanoparticles by using self-assembled biointegrated block copolymers. *Proc. Natl. Acad. Sci. USA* **2008**, *105* (7), 2586-2591.
67. Hrkach, J.; Von Hoff, D.; Mukkaram Ali, M.; Andrianova, E.; Auer, J.; Campbell, T.; De Witt, D.; Figa, M.; Figueiredo, M.; Horhota, A.; Low, S.; McDonnell, K.; Peeke, E.; Retnarajan, B.; Sabnis, A.; Schnipper, E.; Song, J. J.; Song, Y. H.; Summa, J.; Tompsett, D.; Troiano, G.; Van Geen Hoven, T.; Wright, J.; LoRusso, P.; Kantoff, P. W.; Bander, N. H.; Sweeney, C.; Farokhzad, O. C.; Langer, R.; Zale, S., Preclinical development and

- clinical translation of a PSMA-targeted docetaxel nanoparticle with a differentiated pharmacological profile. *Sci. Transl. Med.* **2012**, *4* (128), 128ra39.
68. Kolishetti, N.; Dhar, S.; Valencia, P. M.; Lin, L. Q.; Karnik, R.; Lippard, S. J.; Langer, R.; Farokhzad, O. C., Engineering of self-assembled nanoparticle platform for precisely controlled combination drug therapy. *P Proc. Natl. Acad. Sci. USA* **2010**, *107* (42), 17939-17944.
69. Mamo, T.; Moseman, E. A.; Kolishetti, N.; Salvador-Morales, C.; Shi, J.; Kuritzkes, D. R.; Langer, R.; von Andrian, U.; Farokhzad, O. C., Emerging nanotechnology approaches for HIV/AIDS treatment and prevention. *Nanomed. Nanotechnol.* **2010**, *5* (2), 269-285.
70. Wang, A. Z.; Gu, F.; Zhang, L.; Chan, J. M.; Radovic-Moreno, A.; Shaikh, M. R.; Farokhzad, O. C., Biofunctionalized targeted Nanoparticles for therapeutic applications. *Expert Opin. Biol. Th.* **2008**, *8* (8), 1063-1070.
71. Zhang, L.; Chan, J. M.; Gu, F. X.; Rhee, J. W.; Wang, A. Z.; Radovic-Moreno, A. F.; Alexis, F.; Langer, R.; Farokhzad, O. C., Self-assembled lipid-polymer hybrid nanoparticles: a robust drug delivery platform. *ACS Nano* **2008**, *2* (8), 1696-1702.
72. Zhang, L.; Radovic-Moreno, A. F.; Alexis, F.; Gu, F. X.; Basto, P. A.; Bagalkot, V.; Jon, S.; Langer, R. S.; Farokhzad, O. C., Co-delivery of hydrophobic and hydrophilic drugs from nanoparticle-aptamer bioconjugates. *ChemMedChem* **2007**, *2* (9), 1268-1271.
73. Acharya, S.; Sahoo, S. K., PLGA nanoparticles containing various anticancer agents and tumour delivery by EPR effect. *Adv. Drug Delivery Rev.* **2011**, *63* (3), 170-183.
74. Knop, K.; Hoogenboom, R.; Fischer, D.; Schubert, U. S., Poly (ethylene glycol) in drug delivery: pros and cons as well as potential alternatives. *Angew.Chem. Int. Edit.* **2010**, *49* (36), 6288-6308.

75. Maeda, H., The enhanced permeability and retention (EPR) effect in tumor vasculature: the key role of tumor-selective macromolecular drug targeting. *Adv. Enzyme Regul.* **2001**, *41* (1), 189-207.
76. Maeda, H.; Matsumura, Y., Tumoritropic and lymphotropic principles of macromolecular drugs. *Crit. Rev. Ther. Drug* **1988**, *6* (3), 193-210.
77. Matsumura, Y.; Maeda, H., A new concept for macromolecular therapeutics in cancer chemotherapy: mechanism of tumoritropic accumulation of proteins and the antitumor agent smancs. *Cancer Res.* **1986**, *46* (12 Part 1), 6387-6392.
78. Yuan, F.; Dellian, M.; Fukumura, D.; Leunig, M.; Berk, D. A.; Torchilin, V. P.; Jain, R. K., Vascular permeability in a human tumor xenograft: molecular size dependence and cutoff size. *Cancer Res.* **1995**, *55* (17), 3752-3756.
79. Couvreur, P.; Vauthier, C., Nanotechnology: intelligent design to treat complex disease. *Pharm. Res.* **2006**, *23* (7), 1417-1450.
80. Torchilin, V. P., Recent advances with liposomes as pharmaceutical carriers. *Nat. Rev. Drug Discov.* **2005**, *4* (2), 145-160.
81. Hobbs, S. K.; Monsky, W. L.; Yuan, F.; Roberts, W. G.; Griffith, L.; Torchilin, V. P.; Jain, R. K., Regulation of transport pathways in tumor vessels: role of tumor type and microenvironment. *Proc. Natl. Acad. Sci.* **1998**, *95* (8), 4607-4612.
82. Maeda, H., Vascular permeability in cancer and infection as related to macromolecular drug delivery, with emphasis on the EPR effect for tumor-selective drug targeting. *Proc. Jpn. Acad B-Phys.* **2012**, *88* (3), 53.
83. Ferrari, M., Cancer nanotechnology: opportunities and challenges. *Nat. Rev. Cancer* **2005**, *5* (3), 161-171.

84. Gottesman, M. M.; Fojo, T.; Bates, S. E., Multidrug resistance in cancer: role of ATP-dependent transporters. *Nat. Rev. Cancer* **2002**, *2* (1), 48-58.
85. Peer, D.; Margalit, R., Fluoxetine and reversal of multidrug resistance. *Cancer Lett.* **2006**, *237* (2), 180-187.
86. Warenius, H.; Galfre, G.; Bleehen, N.; Milstein, C., Attempted targeting of a monoclonal antibody in a human tumour xenograft system. *Eur. J. Cancer Clin. On.* **1981**, *17* (9), 1009-1015.
87. Gabizon, A. A., Pegylated liposomal doxorubicin: metamorphosis of an old drug into a new form of chemotherapy. *Cancer Invest.* **2001**, *19* (4), 424-436.
88. Wilson, D. S.; Szostak, J. W., In vitro selection of functional nucleic acids. *Annu. Rev. Biochem.* **1999**, *68* (1), 611-647.
89. Schneider, D.; Tuerk, C.; Gold, L., Selection of high affinity RNA ligands to the bacteriophage R17 coat protein. *J. Mol. Biol.* **1992**, *228* (3), 862-869.
90. Irvine, D.; Tuerk, C.; Gold, L., SELEXION: Systematic evolution of ligands by exponential enrichment with integrated optimization by non-linear analysis. *J. Mol. Biol.* **1991**, *222* (3), 739-761.
91. Antony, A., The biological chemistry of folate receptors. *Blood* **1992**, *79* (11), 2807-2820.
92. Unanue, E. R., Secretory function of mononuclear phagocytes: a review. *Am. J. Pathol.* **1976**, *83* (2), 396.
93. Storm, G.; Belliot, S. O.; Daemen, T.; Lasic, D. D., Surface modification of nanoparticles to oppose uptake by the mononuclear phagocyte system. *Adv. Drug Delivery Rev.* **1995**, *17* (1), 31-48.

94. Fang, C.; Shi, B.; Pei, Y.-Y.; Hong, M.-H.; Wu, J.; Chen, H.-Z., In vivo tumor targeting of tumor necrosis factor- α -loaded stealth nanoparticles: Effect of MePEG molecular weight and particle size. *Eur. J. Pharm. Sci.* **2006**, 27 (1), 27-36.

CHAPTER 2

IMMUNE STIMULATING PHOTOACTIVE HYBRID NANOPARTICLES FOR
METASTATIC BREAST CANCER

Reprinted with permission from Marrache, S.; Choi, J. H.; Tundup, S.; Zaver, D.; Harn, D.;
Dhar, S. *Integr. Biol.*, 5, 215. Copyright 2013, Royal Society of Chemistry.

Abstract

A therapeutic technology that combines the phototoxic and immune-stimulating ability of photodynamic therapy (PDT) with the widespread effectiveness of the immune system could be promising in the treatment of metastatic breast cancer. We speculate that knowledge of the molecular mechanisms of existing multi-component therapies could provide clues to aid the discovery of new combinations of an immunostimulant with a photosensitizer (PS) using a nanoparticle (NP) delivery platform. Challenges when administering therapeutic combinations include the choice of dosages to reduce side effects, the definitive delivery of the correct drug ratio, and exposure to the targets of interest. These goals are difficult to achieve when drugs are administered individually. By combining controlled-release polymer-based NP drug delivery approaches, we were able to differentially deliver a zinc phthalocyanine (ZnPc)-based PS to metastatic breast cancer cells in combination with CpG-ODN, a single-stranded DNA that is a known immunostimulant to manage distant tumors in a temporally regulated manner. We encapsulated ZnPc which is a long-wavelength absorbing PS within a polymeric NP core made up of poly(D,L-lactic-*co*-glycolic acid)-*b*-poly(ethylene glycol) (PLGA-*b*-PEG). After coating the outside of the polymeric core with gold NPs (AuNPs), we further modified the AuNP surface with CpG-ODN. *In vitro* cytotoxicity using 4T1 metastatic mouse breast carcinoma cells shows significant photocytotoxicity of the hybrid NPs after irradiation with a 660 nm LASER light. This activity in these hybrids, which contained both ZnPc and CpG-ODN, was remarkably better than with either treatment alone. Treatment of mouse bone marrow-derived dendritic cells with the PDT-killed 4T1 cell lysate shows that the combination of PDT with a synergistic immunostimulant in a single NP system results in a significant immune response that can be used to treat metastatic cancer.

Introduction

Management of metastatic breast cancer remains a therapeutic challenge¹. An ideal cancer treatment should not only cause tumor regression and eradication but also induce a systemic antitumor immunity for control of metastatic tumors and long-term tumor resistance. This can be achieved by using the immune system as a weapon that recognizes the tumor antigen so that once the primary tumor is eliminated, metastases will also be destroyed. Earlier success in applying the immune system to metastatic cancer, as well as the limited contributions from conventional chemo or radiation therapy, makes metastatic cancer a focus for contemporary development of novel treatment options². The main pillars of cancer treatment-chemotherapy, surgery, and radiation therapy- are known to suppress the immune system³. The only known cancer treatment that stimulates anti-tumor immunity is photodynamic therapy (PDT)^{3,4}. PDT involves administration of a photosensitizer (PS) followed by illumination of the tumor with a long wavelength (600-800 nm) light. This illumination produces a reactive oxygen species (ROS), resulting in vascular shutdown, cancer cell apoptosis, and the induction of a host immune response⁵. The exact mechanism involved in the PDT-mediated induction of anti-tumor immunity is not yet understood. Possible mechanisms include alterations in the tumor microenvironment by stimulating pro-inflammatory cytokines and direct effects of PDT on the tumor that increase immunogenicity³. PDT can increase maturation and differentiation of dendritic cells (DCs), which then lead to the generation of tumor specific cytotoxic CD8 T cells that can destroy distant deposits of untreated tumor^{3,6-8}(Figure2.1.).

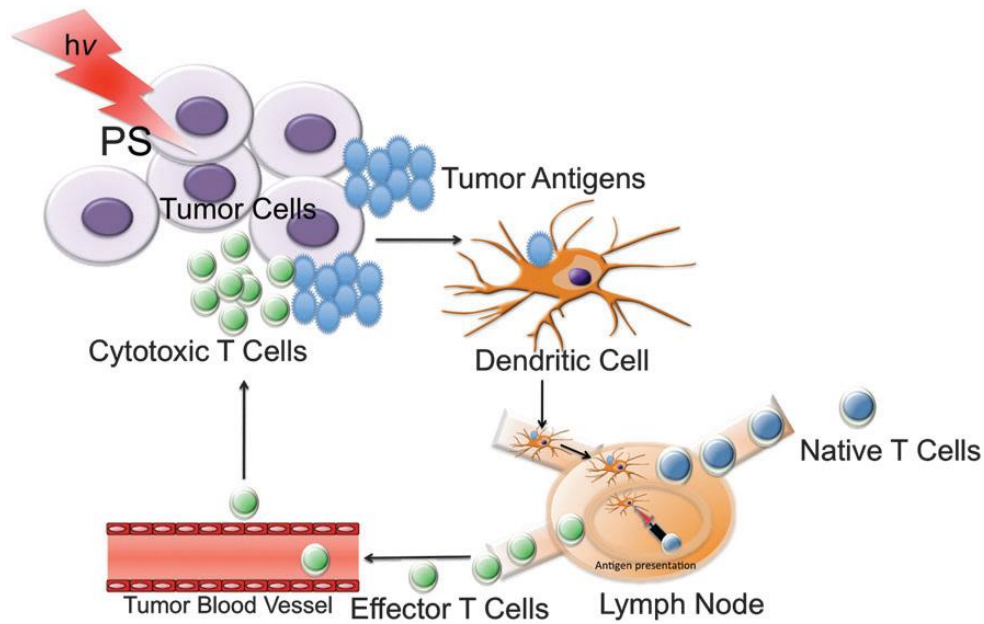


Figure 2.1. Phagocytosis of tumor antigens by DCs after PDT.

An increasing number of studies show that immunoadjuvants injected intratumorally can produce a similar infiltration of leukocytes into the tumor³. Immunoadjuvants are frequently prepared from microbial cells and are thought to act *via* toll-like receptors (TLRs)⁹ present on macrophages and DCs. This indicates that a combination of PDT with a DC activating agent that can act as an agonist of TLR might be promising for the treatment of metastatic tumor. There are few reports of combinations of PDT with microbial derived products potentiating tumor response and leading to long-term anti-tumor immunity^{3, 10}. However, thus far administration of immunoadjuvants as separate constructs by intratumoral injection has only been explored to combine PDT with immunotherapy^{11, 12}, their use as a single construct should receive careful consideration. Nanotechnology-based differential combination therapy can be emphasized as a promising strategy for metastatic breast cancer. By combining controlled release nanoparticles (NPs), PDT, and immune activation, we aimed to differentially deliver PS with synergistic immunoadjuvants in a temporally regulated manner. Polymeric NPs of poly(lactic-*co*-glycolic

acid)-*b*-poly(ethylene glycol) (PLGA-*b*-PEG) block copolymers are especially promising as drug delivery vehicles¹³⁻¹⁵. The use of PLGA and PEG polymers in FDA-approved products makes these biomaterials ideal for the development of new therapeutics. We used zinc(II) phtahlocyanine (ZnPc)¹⁶ as a PS because of its high optical absorption coefficient in the 600 to 800 nm phototherapeutic window, which is higher than the FDA-approved PDT drug, photofrin®. We encapsulated the PS inside PLGA-*b*-PEG polymeric NPs and modified the surface of the polymeric core with gold NPs (AuNPs) by using noncovalent interactions. For immune stimulation, the surface of the AuNPs was used to introduce 5'-purine-purine/T-CpG-pyrimidine-pyrimidine-3'-oligodeoxynucleotides (CpG-ODN) as a potent DC activating agent¹⁷.

¹⁸. Figure 2.2 is a highly advanced biodegradable hybrid NP platform for a proof-of-concept demonstration of such a technology.

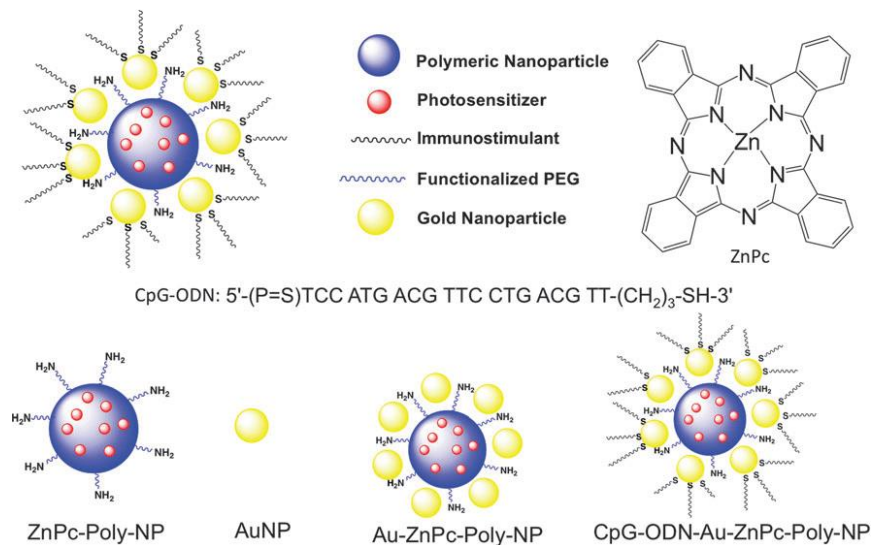


Figure 2.2. Schematic diagram of the NP platform for combination therapy of metastatic breast cancer.

Experimental

Materials

All chemicals were used without further purification unless otherwise noted. PLGA-COOH of inherent viscosity of 0.18 dL/g was purchased from Lactel. NH₂-PEG-NH₂ (MW 2000) was obtained from JenKem USA. 4-dimethylaminopyridine (DMAP), N,N'-dicyclohexylcarbodiimide (DCC), and 3-(4,5-dimethylthiazol-2-yl)-2,5-diphenyltetrazolium bromide (MTT) were purchased from Sigma-Aldrich. AuNPs of size 5 nm (5×10^{13} particles/mL) were purchased from BBInternational. Phosphorothioate oligonucleotide CpG-ODN-1826 of sequence 5'-TCCATGACGTTCTGACGTT-3' was purchased from Midland Certified Reagent Company (Midland, Tex.). Granulocyte-macrophage colony-stimulating factor (GM-CSF) was purchased from R&D Systems. Cytokines were tested using BD OptEIA mouse enzyme-linked immunosorbent assay (ELISA) kits. Distilled water was purified by passage through a Millipore Milli-Q Biocel water purification system (18.2 M Ω) containing a 0.22 μ m filter. Dynamic light scattering (DLS) measurements for size, zeta potential, and polydispersity index (PDI) were carried out using a Malvern Zetasizer Nano ZS system. ¹H and ¹³C NMR spectra were recorded on a 400 MHz Varian NMR spectrometer. Gel permeation chromatographic (GPC) analyses were performed on Shimadzu LC20-AD prominence liquid chromatographer equipped with a RI detector, molecular weights were calculated using a conventional calibration curve constructed from narrow polystyrene standards. Optical measurements were carried out on a NanoDrop 2000 spectrophotometer. HPLC analyses were made on an Agilent 1200 series instrument equipped with a multi-wavelength UV-visible detector. Transmission electron microscopy (TEM) images were taken in a FEI Tecnai 20 TEM

microscope. LASER irradiation was performed in a dark environment using a Melles Griot 660 nm 56 ICS series diode laser equipped with a fiber optic cable.

Cell Line and Cell Culture

The BALB/c mammary adenocarcinoma 410.4 sub-line 4T1 cells from the American Type Culture Collection (ATCC) were grown in RPMI 1640 media containing HEPES, glutamine, sodium pyruvate, 10% fetal bovine serum (FBS), 100 U/mL penicillin, and 100 μ g/mL streptomycin at 37 °C in 5% CO₂. Cells were passed every 3 days and restarted from the frozen stocks upon reaching pass number 20.

Animals

Animals used in the experiments were obtained from Jackson Laboratory and handled in accordance with "The guide for the Care and Use of Laboratory Animals" of American Association for Accreditation of Laboratory Animal Care (AALAC), Animal Welfare Act (AWA), and other applicable federal and state guidelines. All animal work presented here was approved by Institutional Animal Care and Use Committee (IACUC) of University of Georgia.

Synthesis of PLGA-*b*-PEG-NH₂

PLGA-*b*-PEG-NH₂ was synthesized by using an amide coupling reaction. NH₂-PEG-NH₂ (0.7 g, 0.35 mmol), PLGA-COOH (0.8 g, 0.12 mmol), and DMAP (0.16 g, 1.32 mmol) in 10 mL dry CH₂Cl₂ was set to stir on ice. DCC (34.1 mg, 0.17 mmol) in 1 mL dry CH₂Cl₂ was added drop wise to the solution. The solution was warmed to room temperature and stirred overnight. It was then filtered to remove the dicyclohexylurea byproduct, precipitated using a mixture of 50:50 methanol-diethyl ether, isolated via centrifugation (5000 rpm, 4 °C, 10 min), and lyophilized overnight. PLGA-*b*-PEG-NH₂ was isolated as a white solid in 29% yield. ¹H NMR (CHCl₃-*d*): δ 5.3 [m, (OCHCH₃C(O))], 4.9 [m, (OCH₂C(O))], 3.6 [s, (OCH₂CH₂)], 1.9 [m,

(CH_3CH)]. ^{13}C NMR ($CHCl_3-d$): δ 169.6, 166.5, 66.0, 61.1, 60.9, 16.9, 15.5. GPC: $M_n = 7,070$ g/mol, $M_w = 8,540$ g/mol, PDI = 1.21.

Synthesis of ZnPc-Poly-NPs

ZnPc-encapsulated NPs (ZnPc-Poly-NPs) were prepared by using the nanoprecipitation method.¹⁹ PLGA-*b*-PEG-NH₂ (50 mg/mL) and ZnPc, at varying percent weight with respect to the polymer weight, were dissolved in DMF. This mixture was slowly added to water over a period of 10 min. The NPs formed were stirred at room temperature for 2-3 h and washed 3 times with nanopure water using Amicon ultracentrifugation filtration membranes with a molecular weight cutoff of 100 kDa (3000 rpm, 4 °C). The NP size, PDI, and zeta potential were obtained by DLS measurements. Size and the morphology of the NPs were further confirmed by TEM. The ZnPc content in the NPs was measured by HPLC.

Synthesis of Au-ZnPc-Poly-NPs

An aqueous suspension of 1 mL ZnPc-Poly-NPs was added to a 2 mL aqueous solution of citrate coated AuNPs of size 5 nm and allowed to sit for 4 h at room temperature. The NPs were characterized by DLS, TEM, and UV-Vis spectroscopy.

Synthesis of CpG-ODN-Au-ZnPc-Poly-NPs

CpG-ODN of sequence 5'-TCCATGACGTTTCCTGACGTT-3' with a disulfide bond in the 5' end was deprotected according to the manufacturer's protocol. Briefly, an aqueous solution of 0.1 M DTT was added to a solution of CpG-ODN in 0.1 M triethylammonium acetate buffer (pH 6.5), and incubated at room temperature for 30 min. The deprotected CpG-ODN was purified using a 50 mg C18 Sep-Pak cartridge (Waters, Milford, MA) equilibrated in and eluted with DNase/RNase-free distilled water. The concentration of the CpG-ODN was measured by UV-Vis spectroscopy. Au-ZnPc-Poly-NPs were added to an equivalent volume of 10% (v/v)

Tween 20 at room temperature. Then CpG-ODN was added (210 μ L, 105 μ g/mL) and incubated at room temperature in a shaker for 20 h. CpG-ODN-Au-ZnPc-Poly-NPs were washed 3 times using Amicon ultracentrifugation filtration membranes with a molecular weight cutoff of 100 kDa (3000 rpm, 4 $^{\circ}$ C). Finally, NPs were resuspended in water and analyzed by DLS. NP solutions were analyzed by UV-Vis after dissolving the polymeric core using 1 M NaOH for determination of encapsulated ZnPc content or dissolving the gold core with 0.6 M KI for quantification of conjugated CpG-ODN.

Determination of ZnPc loading and encapsulation efficiency

ZnPc loading and encapsulation efficiency (EE) were calculated by dissolving the polymer core by mixing equal portions of the NP solution and 1 N NaOH, followed by dilution with a 50:50 water:acetonitrile mixture, and subsequent HPLC analysis (wavelength: 670 nm). ZnPc loading is defined as the mass fraction of PS in the NPs, whereas EE is the fraction of initial PS used for encapsulation by the NPs during nanoprecipitation²⁰.

MTT Assay

The phototoxic behavior of all the NPs was evaluated using the MTT assay against 4T1 cells. 4T1 cells (1500 cells/well) were seeded on a 96-well plate in 100 μ L of RPMI medium and incubated for 24 h. The cells were treated with NPs at varying concentrations (with respect to ZnPc) and incubated for 2 h at 37 $^{\circ}$ C. The cells were then irradiated with a 660 nm LASER (power 20 mW) with fiber optics for 5 min per well. Irradiated cells were incubated for 12 h at 37 $^{\circ}$ C, the medium was changed after 12 h, and the cells were incubated for an additional 60 h. The cells were then treated with 20 μ L of MTT (5 mg/mL in PBS) for 5 h. The medium was removed, the cells were lysed with 100 μ L of DMSO, and the absorbance of the purple formazan was recorded at 550 nm using a Bio-Tek Synergy HT microplate reader. Each well was

performed in triplicate. All experiments were repeated three times. Cytotoxicity was expressed as mean percentage increase relative to the unexposed control \pm SD. Control values were set at 0% cytotoxicity or 100% cell viability. Cytotoxicity data (where appropriate) was fitted to a sigmoidal curve and a three parameters logistic model was used to calculate the IC₅₀, which is the concentration of the agent causing 50% inhibition in comparison to untreated controls. The mean IC₅₀ is the concentration of agent that reduces cell growth by 50% under experimental conditions and is the average from at least three independent measurements that were reproducible and statistically significant. The IC₅₀ values are reported at \pm 95% confidence intervals (\pm 95% CI). This analysis was performed with Graph Pad Prism (San Diego, U.S.A) software.

Results and Discussions

Synthesis of the polymer and construction of the NPs

To co-deliver PS and an immunoadjuvant using a single NP construct and to obtain adequate control over encapsulation of the hydrophobic PS, ZnPc, we synthesized a biodegradable polymer with a terminal -NH₂ group (PLGA-*b*-PEG-NH₂) via an amide coupling of PLGA-COOH with NH₂-PEG-NH₂ using DCC/DMAP as coupling agents. This polymer was characterized by ¹H and ¹³C NMR spectroscopy (Figure 2.3.). Purity, molecular weights, and the PDI of the polymer were determined by GPC measurements using tetrahydrofuran mobile phase (Table 2.1.). These results are consistent with previously reported data for a PLGA-*b*-PEG-COOH polymer²¹.

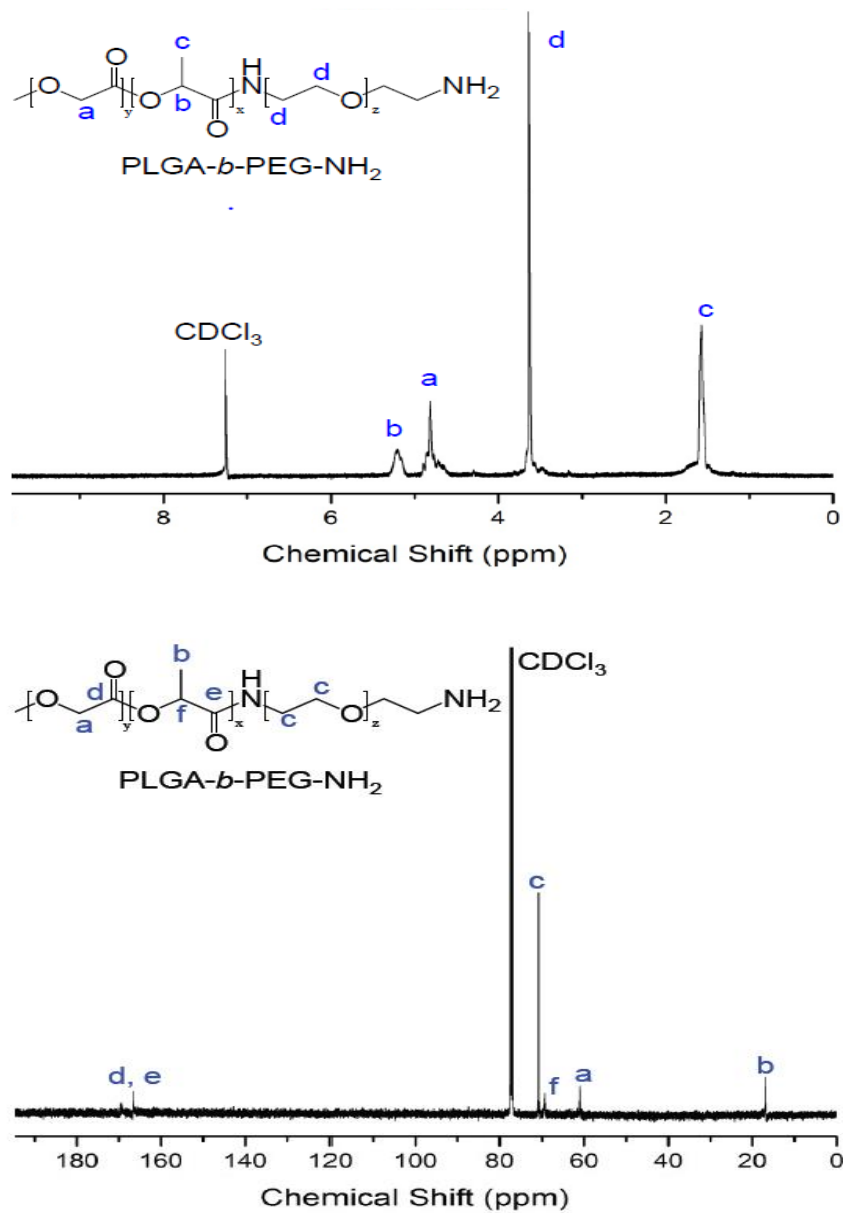


Figure.2.3. ¹H and ¹³C NMR of PLGA-*b*-PEG-NH₂

Table 2.1. Comparison of molecular weights of PLGA-COOH and PLGA-*b*-PEG-NH₂ as determined from gel permeation chromatographic (GPC)

Molecular Weight	PLGA-COOH	PLGA- <i>b</i> -PEG-NH ₂
M _w	6,750 g/mol	8,540 g/mol
M _n	4,300 g/mol	7,070 g/mol
PDI	1.57	1.21

Synthesis of the NPs with PLGA-*b*-PEG-NH₂ was achieved by the nanoprecipitation method.^{19, 22} PLGA-*b*-PEG-NH₂ was dissolved in a water miscible solvent DMF and then added drop wise into an aqueous solution, thereby generating NPs. The properties of the encapsulated NPs were characterized by DLS to find the hydrodynamic diameter, zeta potential, and PDI of each preparation. To optimize size and loading, a series of encapsulated NPs was prepared by varying the weight percentage of ZnPc to polymer (%w/w) and by using the PEG of various molecular masses. When the DMF solution of the polymer and ZnPc was added to water, the mixture became turbid, indicating the formation of NPs. However, depending on the conditions, the final suspension contained a larger or smaller amount of larger polymeric aggregates either dispersed in the aqueous phase or adhering to the flask wall or to the magnetic stirring bar. In this way, we found that the PLGA of the inherent viscosity of 0.18 dL/g in hexafluoroisopropanol affords the most suitable encapsulated NPs. It is worth noting that measurements of NP size made on three different batches produced under identical conditions fell within a range of 10% variation, indicating good reproducibility. The loading efficiencies of ZnPc at various added weight percentages with respect to the polymer weight are given in Table

2.2. The size of the NPs increased with ZnPc loading (Table 2.2.). For all in vitro studies, we used encapsulated NPs containing 30% ZnPc added with respect to the polymer.

Table 2.2. Loading efficiencies of ZnPc at various weight percentage with respect to the polymer.

Wt % of ZnPc	Diameter (nm)	PDI	Zeta Potential (mv)	% loading
0	92 ± 1	0.33	16.0 ± 3.5	0
5	104 ± 7	0.36	3.8 ± 2.4	3
10	101 ± 0.5	0.27	17.6 ± 0.5	8
20	117 ± 10	0.25	9.0 ± 1.4	20
30	120 ± 6	0.29	6.9 ± 3.3	20

To synthesize the hybrid NPs, we used AuNPs stabilized with anionic ligand citrate. This allowed an effective binding between the positively charged NH₂ groups of the polymeric ZnPc-Poly-NPs and the negatively charged citrate groups of the AuNPs. The formation of these hybrid Au-ZnPc-Poly-NPs was evident from the DLS measurement. This measurement shows a change in value from positive to negative in the zeta potential of the polymeric NPs (Figure 2.5.). The addition of ZnPc-Poly-NPs to AuNPs did not cause any aggregation (Figure 2.4.).

We modified the AuNP surface with CpG-ODN with a 5'-modified -SH group²³. We were able to load a high concentration of CpG-ODN on the AuNP surface as evident from the UV-Vis study (Figure 2.6.). CpG-ODN adsorption stabilized the hybrid NPs, and the steric repulsion of the NPs prevented flocculation as evidence by the decrease in size and PDI (Figure 2.5.). The negative zeta potential of Au-ZnPc-Poly-NPs decreased with formation of the CpG-ODN-Au-ZnPc-Poly-NPs. TEM images are another evidence of formation of the hybrid NPs (Figure 2.7.).

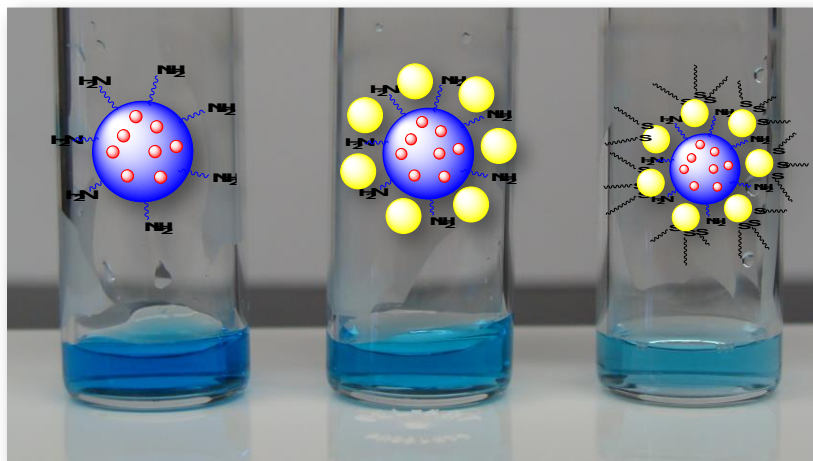


Figure 2.4. Photographs of NP suspensions with no visible aggregation.

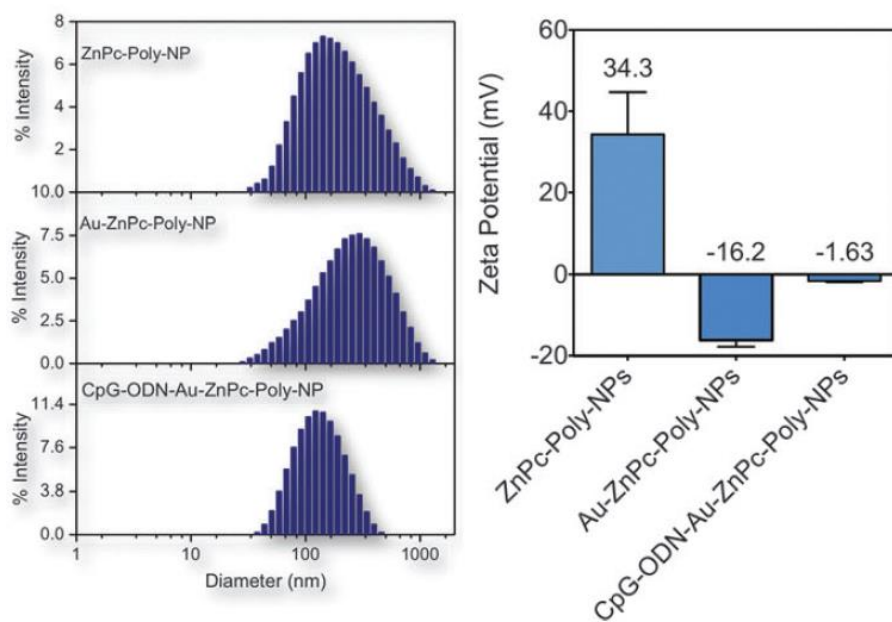


Figure 2.5. Hydrodynamic diameter and zeta potential of the NPs by DLS measurements.

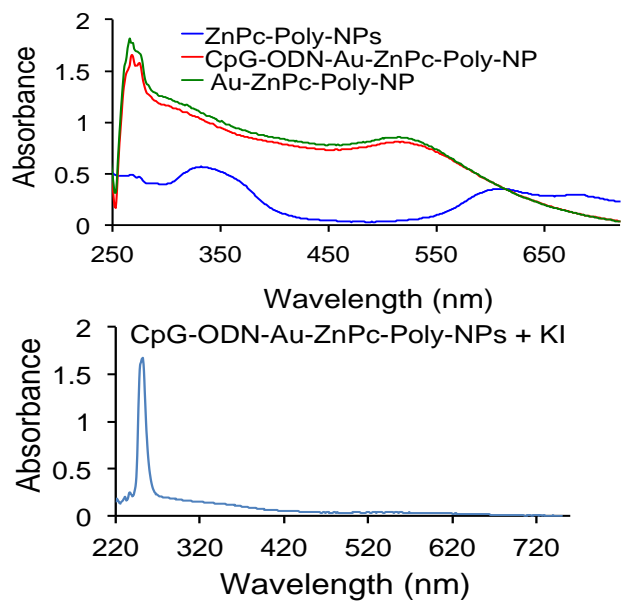


Figure 2.6. Characterization of hybrid NPs by UV-VIS spectroscopy

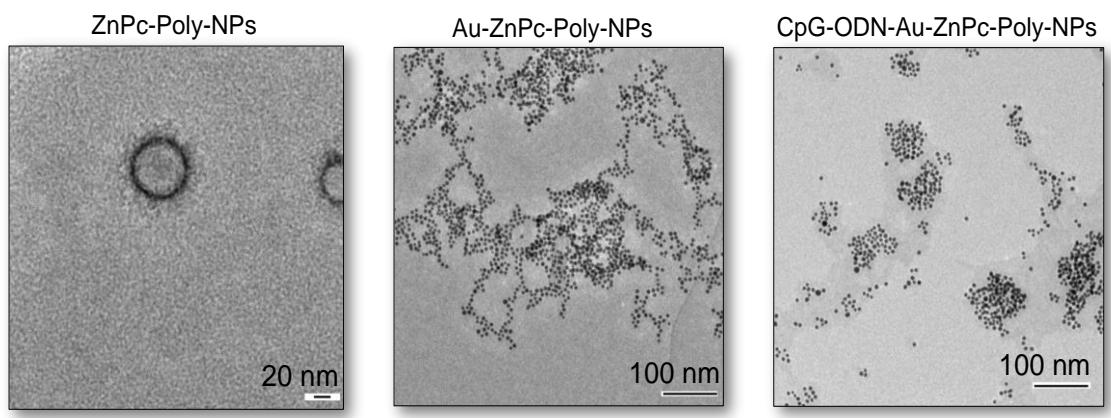


Figure 2.7. TEM images of ZnPc-Poly-NPs, Au- ZnPc-Poly-NPs, and CpG-ODN-Au- ZnPc-Poly-NPs.

***In vitro* stability of the hybrid NPs**

In vitro stability of NPs can be defined relative to changes in their hydrodynamic size and surface charge in response to changes in the sample environment. Their key physicochemical properties, nanoparticle size, surface zeta potential, and morphology determine their *in vivo* stability profiles. We checked the short-term stability of an aqueous suspension of CpG-ODN-Au-ZnPc-Poly-NPs by storing it at 4 °C for 30 days and then evaluating the size distribution and zeta potential (Table 2.3.). The diameter of the hybrid NPs decreased. The mean size decreased from 186 nm to ~90 nm after 30 days and the surface charge changes from ~ -10 mV to -20 mV (Table2.3.).

Table 2.3. Stability of CpG-ODN-Au-ZnPc-Poly-NPs by DLS measurements in nanopure water

	Diameter (nm)	PDI	Zeta Potential (mV)
Day 1	186.0 ± 4.5	0.53 ± 0.07	-10.6 ± 0.4
Day 30	90.0 ± 0.4	0.42 ± 0.01	-20.5 ± 0.3

***In vitro* phototoxicity on metastatic breast cancer cells**

The photodynamic activities of ZnPc-Poly-NPs, Au-ZnPc-Poly-NPs, and CpG-ODN-Au-ZnPc-Poly-NPs were investigated against the 4T1 cell line using a 660 nm laser. Cells were incubated with all the constructs without illumination to serve as dark controls (Figure.2.8.). None of these constructs showed any phototoxicity in the dark. The induction of cell death was both light and ZnPc-dose dependent. Two hours after the incubations, cells were illuminated with a 660 nm LASER light for 5 min per well. The mortality of post-PDT cultures was determined after the MTT assay. A higher phototoxic effect was observed with CpG-ODN-Au-

ZnPc-Poly-NPs (IC_{50} ; 2.8 nM) than the ZnPc-Poly-NPs (IC_{50} ; 15 nM), Au-ZnPc-Poly-NPs (IC_{50} ; 6 nM) or free ZnPc (IC_{50} ; 317 nM). Control cells incubated with unconjugated AuNPs did not display any significant cell death after illumination. Thus, under these in vitro conditions we can exclude the possibility that photothermal activity of the AuNPs causes any case of cell death. Interestingly, the efficacy of free ZnPc was lower than that for hybrid NPs containing ZnPc in the polymeric core and CpG-ODN immobilized on the AuNP surface. This enhancement in photodynamic efficacy is likely a consequence of the synergistic effect between ZnPc and CpG-ODN when delivered in a single construct.

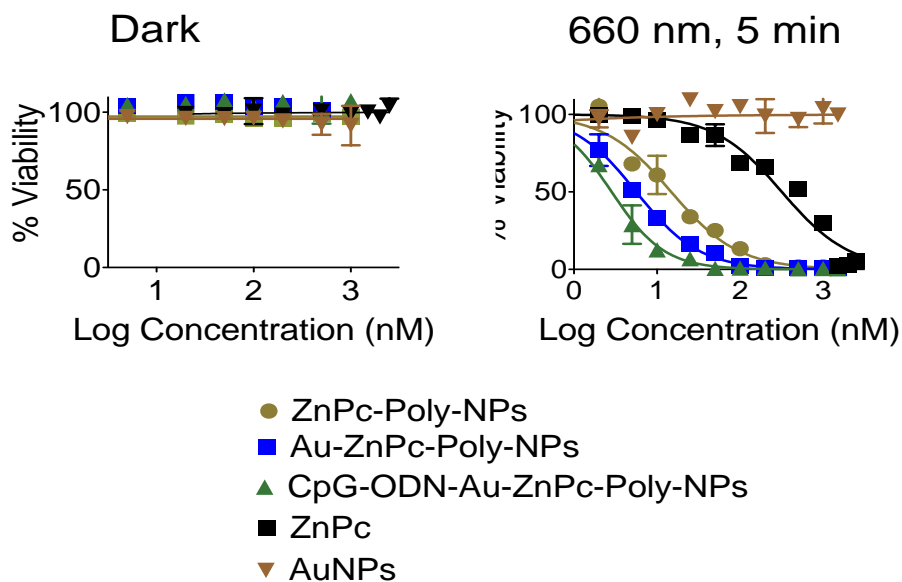


Figure 2.8. Cytotoxicity profiles in 4T1 cells in the dark (left) and after 5 min exposure with a 660 nm Laser (right).

Conclusions

In summary, a hybrid NP system that can be loaded with a photosensitizer and an immunoadjuvant for combination therapy was synthesized. The PLGA-*b*-PEG copolymer

functionalized with a terminal $-NH_2$ group was used to yield a hydrophobic core for effective loading of a photosensitizer, ZnPc. The amine groups from the polymeric NPs, acting as anchors, were used to decorate the NP surface with anionic AuNPs and CpG-ODN-based immunoadjuvant was immobilized on the gold surface. Using 4T1 cells as a model for metastatic breast cancer, the phototoxicity of this hybrid NP containing CpG-ODN and the photosensitizer, ZnPc, is significantly higher than that of the free PS, PS alone in a NP, or a combination of the PS and the immunoadjuvant in their free forms. Several cytokines were involved in the PDT-induced immune response after treatment with CpG-ODN-Au-ZnPc-Poly-NPs. When a mixture of CpG-ODN and ZnPc was used, no significant immune response was seen under similar conditions. These results indicate that the PDT-induced antitumor immune response and its further enhancement by using a synergistic immunoadjuvant in a suitably designed NP construct might play an important role in control of malignant diseases. These results support the concept that a rational choice of an immunostimulant can be an ideal addition to a PDT regimen if both the photosensitizer and the immunoadjuvant can be delivered using a single delivery vehicle. These results will play critical roles in building the knowledge required to design NPs to be used for photoimmunotherapy of metastatic cancers.

References

1. DeSantis, C.; Siegel, R.; Bandi, P.; Jemal, A., Breast cancer statistics, 2011. *CA Cancer J. Clin.* **2011**, *61* (6), 408-418.
2. Turcotte, S.; Rosenberg, S. A., Immunotherapy of Metastatic Solid Cancers. *Adv. surg.* **2011**, *45*, 341.
3. Castano, A. P.; Mroz, P.; Hamblin, M. R., Photodynamic therapy and anti-tumour immunity. *Nat. Rev. Cancer* **2006**, *6* (7), 535-545.
4. Gollnick, S. O.; Owczarczak, B.; Maier, P., Photodynamic therapy and anti-tumor immunity. *Lasers Surg. and Med.* **2006**, *38* (5), 509-515.
5. Dougherty, T. J.; Gomer, C. J.; Henderson, B. W.; Jori, G.; Kessel, D.; Korbek, M.; Moan, J.; Peng, Q., Photodynamic therapy. *J. Natl. Cancer Inst.*, **1998**, *90* (12), 889-905.
6. Korbek, M., Cancer vaccines generated by photodynamic therapy. *Photochem. Photobiol. Sci.* **2011**, *10* (5), 664-669.
7. Van Duijnhoven, F. H.; Aalbers, R. I.; Rovers, J. P.; Terpstra, O. T.; Kuppen, P. J., Immunological Aspects of Photodynamic Therapy of Liver Tumors in a Rat Model for Colorectal Cancer. *Photochem. Photobiol.* **2003**, *78* (3), 235-240.
8. Oseroff, A., PDT as a cytotoxic agent and biological response modifier: implications for cancer prevention and treatment in immunosuppressed and immunocompetent patients. *J. Invest. Dermatol.* **2006**, *126* (3), 542-544.
9. Werling, D.; Jungi, T. W., TOLL-like receptors linking innate and adaptive immune response. *Vet. Immunol. Immunopathol.* **2003**, *91* (1), 1-12.
10. Gollnick, S. O.; Brackett, C. M., Enhancement of anti-tumor immunity by photodynamic therapy. *Immunol. Res.* **2010**, *46* (1-3), 216-226.

11. Qiang, Y. G.; Yow, C.; Huang, Z., Combination of photodynamic therapy and immunomodulation: current status and future trends. *Med. Res. Rev.* **2008**, *28* (4), 632-644.
12. Denis, T. G. S.; Aziz, K.; Waheed, A. A.; Huang, Y.-Y.; Sharma, S. K.; Mroz, P.; Hamblin, M. R., Combination approaches to potentiate immune response after photodynamic therapy for cancer. *Photochem. Photobiol. Sci.* **2011**, *10* (5), 792-801.
13. Dhar, S.; Gu, F. X.; Langer, R.; Farokhzad, O. C.; Lippard, S. J., Targeted delivery of cisplatin to prostate cancer cells by aptamer functionalized Pt (IV) prodrug-PLGA-PEG nanoparticles. *Proc. Natl. Acad. Sci. USA* **2008**, *105* (45), 17356-17361.
14. Farokhzad, O. C.; Jon, S.; Khademhosseini, A.; Tran, T.-N. T.; LaVan, D. A.; Langer, R., Nanoparticle-aptamer bioconjugates a new approach for targeting prostate cancer cells. *Cancer Res.* **2004**, *64* (21), 7668-7672.
15. Soppimath, K. S.; Aminabhavi, T. M.; Kulkarni, A. R.; Rudzinski, W. E., Biodegradable polymeric nanoparticles as drug delivery devices. *J. Controlled Release* **2001**, *70* (1), 1-20.
16. Ochsner, M., Light scattering of human skin: A comparison between zinc (II)—phthalocyanine and photofrin II® . *J. Photochem. Photobiol. B* **1996**, *32* (1), 3-9.
17. Yamamoto, S.; Yamamoto, T.; Nojima, Y.; Umemori, K.; Phalen, S.; McMurray, D. N.; Kuramoto, E.; Iho, S.; Takauji, R.; Sato, Y., Discovery of immunostimulatory CpG-DNA and its application to tuberculosis vaccine development. *Jpn. J. Infect. Dis.* **2002**, *55* (2), 37-44.

18. Weeratna, R. D.; Makinen, S. R.; McCluskie, M. J.; Davis, H. L., TLR agonists as vaccine adjuvants: comparison of CpG ODN and Resiquimod (R-848). *Vaccine* **2005**, *23* (45), 5263-5270.
19. Dhar, S.; Kolishetti, N.; Lippard, S. J.; Farokhzad, O. C., Targeted delivery of a cisplatin prodrug for safer and more effective prostate cancer therapy in vivo. *Proc. Natl. Acad. Sci. USA* **2011**, *108* (5), 1850-5.
20. Karnik, R.; Gu, F.; Basto, P.; Cannizzaro, C.; Dean, L.; Kyei-Manu, W.; Langer, R.; Farokhzad, O. C., Microfluidic platform for controlled synthesis of polymeric nanoparticles. *Nano Lett.* **2008**, *8* (9), 2906-2912.
21. Gu, F.; Zhang, L.; Teply, B. A.; Mann, N.; Wang, A.; Radovic-Moreno, A. F.; Langer, R.; Farokhzad, O. C., Precise engineering of targeted nanoparticles by using self-assembled biointegrated block copolymers. *Proc. Natl. Acad. Sci.* **2008**, *105* (7), 2586-2591.
22. Dhar, S.; Gu, F. X.; Langer, R.; Farokhzad, O. C.; Lippard, S. J., Targeted delivery of cisplatin to prostate cancer cells by aptamer functionalized Pt(IV) prodrug-PLGA-PEG nanoparticles. *Proc Natl Acad Sci USA* **2008**, *105* (45), 17356-17361.
23. Dhar, S.; Daniel, W. L.; Giljohann, D. A.; Mirkin, C. A.; Lippard, S. J., Polyvalent oligonucleotide gold nanoparticle conjugates as delivery vehicles for platinum (IV) warheads. *J. Am. Chem. Soc.* **2009**, *131* (41), 14652-14653.

CHAPTER 3

CHEMO-ANTI-INFLAMMATORY THERAPY FOR CANCER

Introduction

Inflammation is closely related to tumorigenesis. Chronic inflammation plays an significant role in approximately 20% of human cancers¹. The inflammatory genes and cytokines found in tumors contribute to tumor growth, progression, and immunosuppression. Moreover, deletion or inhibition of inflammatory cytokines prevents tumor development². Nuclear factor kappa B (NF- κ B) is an one of the inflammatory genes that is a central regulator of the inflammatory response³. Activation of NF- κ B promotes cell proliferation while down regulation presents the opposite effect; thus NF- κ B is one of major factor in tumorigenesis⁴⁻⁷.

Cis-diamminedichloridoplatinum(II), or cisplatin^{8,9}, is currently one of the most effective anticancer drugs available to treat a variety of solid tumors¹⁰. Despite the great success in treating cancer, the efficiency of cisplatin is compromised by its induction of numerous unpleasant side effects and acquired resistance to its effectiveness¹¹⁻¹⁵.

Because of the limitations, use of anti-inflammatory drugs such as aspirin, ibuprofen, and naproxen, member of nonsteroidal anti-inflammatory drugs(NSAIDs), and curcumin can be an attractive addition to chemotherapeutic approaches due to their ostensive potential in cancer chemoprevention¹⁶.

The primary target of NSAIDs is cyclooxygenase (COX) isoforms, COX-1 and COX-2, which catalyze the rate-limiting step in the formation of prostaglandins (PGs). PGs are a group of

lipid molecules derived from arachidonic acid and play a key role in generating inflammatory responses. The inducible isoform COX-2 and its products, especially PGE₂, are involved in inflammatory responses, inhibition of apoptosis, and induction of resistance. Acetylsalicylic acid, or aspirin, which is known to inhibit COX-1 and COX-2 irreversibly through transesterification between acetylsalicylic acid and the Ser-530/516 residue of COX^{17, 18}, also has the potential to reduce the severity of cisplatin-induced side effects related to hearing, balance, and the kidneys¹⁹. Aspirin and its metabolite salicylate induce several anti-inflammatory cytokines to reduce inflammation²⁰⁻²².

Curcumin, a major component of the spice, turmeric, is a nontoxic compound that exhibits anti-cancer, anti-inflammatory, and anti-oxidative properties. Specifically, it plays a critical role in controlling the NF- κ B signaling pathway by inhibiting phosphorylation of the inhibitor of kappa B, thus causing down regulation of NF- κ B^{23, 24}. Curcumin is also a scavenger of free-radical oxidants via H-atom donation and electron transfer, thus exerting an anti-oxidative property²⁵. Although it exhibits multiple functions, its efficacy in preclinical and clinical studies is limited because of its poor water solubility and of its low bioavailability that is a result of its short biological half-life²⁶. To circumvent these problems, delivery vehicles can be used to deliver curcumin to the target rapidly and accurately.

The mitochondria of cancer cells have a higher negative transmembrane potential than normal cells²⁷. Triphenyl phosphonium (TPP) cation is selectively taken up by mitochondria because of its positive charge and lipophilicity. Based on observation, TPP has been used as a targeting moiety for a delivery agent to mitochondria²⁸. Surface modification of the FDA-approved polymer, PLGA-*b*-PEG, with TPP cation is a promising method of delivering payloads into mitochondria.

A combination of cisplatin and aspirin or curcumin can be an attractive strategy for managing cancer. Major obstacles in administering free-drug formulations include the definitive exposure to the targets of interest, individual pharmacokinetics, and biodistribution parameters. These factors are extremely difficult to control when drugs are individually administered. However, construction of a single prodrug containing a drug combination can potentially overcome these challenges. Thus, an alternative way to deliver a therapeutic combination of cisplatin and aspirin is to fabricate a platinum (IV) prodrug that can be reduced to give cisplatin and aspirin or curcumin. With these challenges in mind, we constructed a platinum (IV) prodrug, Platin-A, with the ability to release cisplatin and aspirin and Platin-C, that can be reduced to yield cisplatin and curcumin as part of their respective biological actions.

Experimental

Materials and Instrumentation

All chemicals were received and used without further purification unless otherwise noted. Cisplatin was purchased from Strem Chemicals, Inc. Aspirin, N, N'-dicyclohexylcarbodiimide (DCC), and a hydrogen peroxide solution (30 wt.% in H₂O), (3-(4,5-dimethylthiazol-2-yl)-2,5-diphenyltetrazolium bromide (MTT) were purchased from Sigma-Aldrich. Interleukin (IL)-6, IL-10, and tumor necrosis factor alpha (TNF- α) cytokines were tested using BD OptEIA mouse enzyme-linked immunosorbent assay (ELISA) kits. Ultra-pure lipopolysaccharide (LPS) was purchased from Invivogen, CA, USA. An Alexa Fluor® 488 annexin V/dead cell apoptosis kit was purchased from Invitrogen. COX (ovine) inhibitor screening assay kit (Cayman Chemical Item Number 560101) was procured from Cayman chemical company Ann Arbor, Mi, USA. K₂PtCl₄, was purchased from Sigma Aldrich.

Distilled water was purified by passage through a Millipore Milli-Q Biocel water purification system (18.2 M Ω) containing a 0.22 μ m filter. ^1H and ^{13}C spectra were recorded on 400 MHz Varian NMR spectrometer and ^{195}Pt NMR spectra were recorded on a 500 MHz Varian NMR spectrometer using K_2PtCl_4 as an external standard. Plate reader analyses were performed on a Bio-Tek Synergy HT microplate reader. Electrospray ionization mass spectrometry (ESI-MS) and high-resolution mass spectrometry (HRMS)-ESI were recorded on Perkin Elmer SCIEX API 1 Plus and Thermo Scientific ORBITRAP ELITE instruments, respectively. Matrix-assisted laser desorption/ionization (MALDI)-time of flight (TOF)-mass spectrometry (MS) were carried out on a Bruker Autoflex (TOF) mass spectrometer. FTIR spectra were collected on a Thermo-Nicolet 6700 spectrophotometer equipped with OMNIC software using samples prepared as pressed KBr pellets. High-performance liquid chromatography (HPLC) analyses were made on an Agilent 1200 series instrument equipped with a multi-wavelength UV-visible and a fluorescence detector. Transmission electron microscopy (TEM) images were taken in a FEI Tecnai 20 TEM microscope. Cells were counted using a Countess® Automated Cell Counter procured from Invitrogen Life Technologies.

Cell Lines and Cell Culture

Human prostate cancer cell lines LNCaP, PC3, and DU145, human breast cancer cell line MCF-7, cisplatin resistant human ovarian cancer cell line A2780 CP70, and RAW 264.7 macrophages were procured from the American type culture collection (ATCC). DU145 cells were grown at 37 °C in 5% CO_2 in Eagle's Minimum Essential Medium (EMEM) supplemented with 10% fetal bovine serum (FBS) and 1% penicillin/streptomycin. LNCaP, PC3, MCF-7, A2780 CP70 and RAW 264.7 cells were grown in Roswell Park Memorial Institute (RPMI) 1640

medium supplemented with 10% FBS and 1% penicillin/streptomycin. Cells were passed every 3 to 4 days and restarted from frozen stocks upon reaching pass number 20.

Synthesis of Platin-A

Platin-A was synthesized by Dr. Rakesh K. Pathak. Synthesis details and characterizations can be found in *Angew. Chem. Int. Ed.*, **2014**, 53, 1963-1967.

Synthesis of (1E,6E)-1,7-bis(4-hydroxy-3-methoxyphenyl)hepta-1,6-diene-3,5-dione (Curcumin)

Acetyl acetone (1.026 mL, 10 mmol), vanillin (2.7 g, 20 mmol), trimethyl borate (2.25 mL, 20 mmol) and boron trioxide (0.662 g, 14 mmol) were dissolved in 80 mL of acetonitrile and heated to 65°C. Then, n-butylamine (0.411 mL, 4.15 mmol) was added slowly to the reaction mixture and stirred for 3 h. Next, 8 mL of acetic acid and 40 mL of ethyl acetate were added and stirred for 30 min. The reaction was then cooled to room temperature and 60 mL of 10% acetic acid was added. Precipitate was filtered and recrystallized with ethanol. 40% yield (1.38g produced) ¹H NMR (CDCl₃, 400 MHz): δ ppm, 7.58 (d, 2H), 7.13 (d, 2H), 7.05 (s, 2H), 6.94 (d, 2H), 6.48 (d, 2H), 5.80 (s, 1H), 3.95 (s, 6H). ¹³C NMR (CDCl₃, 200 MHz): δ ppm 183.24, 147.81, 146.75, 140.53, 127.66, 122.88, 121.76, 114.80, 109.61, 109.58, 55.98

Synthesis of 5-(4-((1E,6E)-7-(4-hydroxy-3-methoxyphenyl)-3,5-dioxohepta-1,6-dien-1-yl)-2-methoxyphenoxy)-5-oxopentanoic acid (Curcumin-glutaric acid)

A solution of curcumin (2.010 g, 5.46 mmol) and DMAP (112 mg, 0.92 mmol) in 100 mL tetrahydrofuran (THF) was prepared and triethylamine (1.33 mL, 10.5 mmol) was added. Glutaric anhydride (685 mg, 6 mmol) in 5 mL of THF was added slowly drop wise into the reaction mixture. The reaction was refluxed overnight at 50°C and evaporated. The resulting residue was dissolved with 55 mL of ethyl acetate followed by 15 mL of 1M HCl and stirred for

10 min. The reaction was extracted with nanopure water 3 times, and the organic solvent was evaporated. A column was run for purification. 27% yield (0.71g produced) ^1H NMR (CDCl_3 , 400 MHz): δ ppm, 7.61 (q, 2H), 7.12 (q, 2H), 7.04 (d, 2H), 6.93 (q, 2H), 6.52 (q, 2H), 5.84 (d, 1H), 3.97 (s, 3H), 3.87 (s, 3H), 2.71 (t, 2H), 2.57 (t, 2H), 2.11 (q, 2H). ^{13}C NMR (CDCl_3 , 200 MHz): δ ppm 203.58, 184.49, 181.78, 177.83, 170.74, 151.27, 147.97, 146.78, 141.13, 141.08, 139.36, 134.11, 127.54, 123.17, 123.03, 120.96, 114.83, 111.36, 109.64, 101.51, 55.95, 55.87, 32.89, 32.55, 19.90

Synthesis of 5-(4-((1*E*,6*E*)-7-(4-hydroxy-3-methoxyphenyl)-3,5-dioxohepta-1,6-dien-1-yl)-2-methoxyphenoxy)-5-oxopentanoic anhydride (Curcumin anhydride)

A solution of 5-(4-((1*E*,6*E*)-7-(4-hydroxy-3-methoxyphenyl)-3,5-dioxohepta-1,6-dien-1-yl)-2-methoxyphenoxy)-5-oxopentanoic acid (0.686 g, 1.42 mmol in dry CH_2Cl_2) was prepared and a solution of DCC (0.146 g, 0.71 mmol) in 3 mL of CH_2Cl_2 was added. The reaction mixture was stirred overnight at room temperature. The byproduct, dicyclohexylurea (DCU), was filtered off in a glass filter and washed with a small amount of CH_2Cl_2 . The solvent was evaporated and the resulting residue was taken up in ethyl acetate. The residual DCU was removed by filtering the resulting suspension through a glass filter. The filtrate was evaporated to give anhydride.

Yield 102% (0.694 g produced). ^1H NMR (CDCl_3 , 400 MHz): δ ppm, 7.59 (m, 4H), 7.12 (m, 4H), 7.07 (m, 4H), 6.92 (m, 4H), 6.50 (m, 4H), 5.83 (m, 4H), 3.93 (s, 6H), 3.87 (s, 6H), 2.71 (m, 4H), 2.57 (m, 4H), 2.11 (m, 4H). ^{13}C NMR (CDCl_3 , 200 MHz): δ ppm 203.58, 184.51, 183.02, 181.76, 181.71, 171.15, 170.79, 170.55, 168.68, 151.21, 148.00, 146.81, 141.13, 139.93, 139.33, 139.25, 134.14, 133.96, 124.23, 123.14, 123.01, 120.93, 114.85, 111.39, 109.67, 101.54, 60.39, 55.94, 55.86, 33.96, 32.80, 32.53, 21.04, 19.50, 14.19

Synthesis of diaminodichloroplatinumdiol (*c,c,t*-[Pt(NH₃)₂Cl₂(OH)₂])

Hydrogen peroxide (30 wt%, 60 mL) was added drop wise to a round bottom flask containing cisplatin (1.0 g, 3.33 mmol). The reaction mixture was heated to 75 °C for 5 h. The bright yellow solution was kept at room temperature in the dark overnight to allow crystallization of the product. Yellow crystals were separated by filtration, washed with cold water and dried. Yield 50% (554 mg produced).

Synthesis of 1-diaminodichloro[(5-{4-[(1E,6E)-7-(4-hydroxy-3-methoxyphenyl)-3,5-dioxohepta-1,6-dien-1-yl]-2-methoxyphenoxy}-5-oxopentanoyl)oxy]platino 4-[(1E,6E)-7-(4-hydroxy-3-methoxyphenyl)-3,5-dioxohepta-1,6-dien-1-yl]-2-methoxyphenyl pentanedioate (Pt(IV)(curcumin)₂)

A mixture of *c,c,t*-[Pt(NH₃)₂Cl₂(OH)₂] (47.8 mg, 0.142 mmol) and curcumin anhydride (673 mg, 0.711 mmol) in 30 mL dimethylsulfoxide (DMSO) was stirred for 72 h at room temperature. The reaction mixture was cooled to 15 °C and DMSO was removed by concentrating with multiple diethyl ether washings. The crude product was suspended in acetonitrile and dimethylformamide (4:1 (v/v)) and precipitated with diethyl ether. This process was repeated three times. Finally the product was sonicated with CH₂Cl₂ to dissolve byproducts. Yield 21 % (38 mg). ¹H NMR (DMSO₆, 400 MHz): δ ppm, 9.71 (s, 2H), 7.62 (m, 4H), 7.33 (m, 4H), 7.13 (q, 4H), 7.06 (d, 4H), 6.93 (q, 4H), 6.80 (q, 4H), 6.56 (broad, 2.23H), 3.84 (d, 12H), 2.74 (t, 4H), 2.61 (t, 4H), 2.37 (q, 4H). ¹³C NMR (DMSO₆, 200 MHz): δ ppm 200.83, 183.70, 171.09, 151.58, 150.0, 148.45, 141.36, 134.19, 126.66, 125.1, 123.82, 121.93, 116.16, 112.55, 111.88, 109.99, 56.45, 55.36, 39.97, 39.76, 39.55, 39.34, 32.55, 21.32, 20.48, 20.42.

Synthesis of 4-[(diaminodichlorohydroxyplatino)oxy]-4-oxobutanoic acid (monosuccinato Pt(IV))

A mixture of *c,c,t*-[Pt(NH₃)₂Cl₂(OH)₂] (250 mg, 0.748 mmol) and succinic anhydride (74.8 mg, 0.748 mmol) were dissolved in 20 mL of DMSO and incubated overnight at room temperature. Once the reaction solution turns clear, solution was reduced by adding diethyl ether until the reaction solution is no longer getting reduced. 5 mL of acetone was then added and vortexed to reduce solution to solidify. It was then centrifuged (6000 rpm, 10 min, 5°C) and lyophilized. 70% yield (324 mg produced) ¹H NMR (CDCl₃, 400 MHz): δ ppm, 7.61 (q, 2H), 7.12 (q, 2H), 7.04 (d, 2H), 6.93 (q, 2H), 6.52 (q, 2H), 5.84 (d, 1H), 3.97 (s, 3H), 3.87 (s, 3H), 2.71 (t, 2H), 2.57 (t, 2H), 2.11 (q, 3H).

Synthesis of 4-({diaminodichloro[(5-{4-[(1E,6E)-7-(4-hydroxy-3-methoxyphenyl)-3,5-dioxohepta-1,6-dien-1-yl]-2-methoxyphenoxy}-5-oxopentanoyl)oxy]platino}oxy)-4-oxobutanoic acid (Platin-C)

Mixture of curcumin anhydride (808 mg, 0.847 mmol) and monosuccinato pt(IV) (183 mg, 0.423 mmol) was dissolved in DMF and stirred at room temperature for 72 h. It was then filtered and rotovapped. Product was redissolved in acetonitrile and little volume of DMF. It was then reprecipitated with diethyl ether three times. Dichloromethane was added to precipitant and sonicated three times to get rid of 5-(4-((1E,6E)-7-(4-hydroxy-3-methoxyphenyl)-3,5-dioxohepta-1,6-dien-1-yl)-2-methoxyphenoxy)-5-oxopentanoic acid. It was then dissolved in acetone and centrifuged. Supernatant was reprecipitated with diethyl ether, centrifuged and lyophilized. 45% yield (172 mg produced) ¹H NMR (DMSO₆, 400 MHz): δ ppm, 7.62 (m, 4H), 7.33 (m, 4H), 7.13 (q, 4H), 7.06 (d, 4H), 6.93 (q, 4H), 6.80 (q, 4H), 6.56 (broad, 2.23H), 3.84 (d, 12H), 2.74 (t, 4H), 2.61 (t, 4H), 2.37 (q, 4H). Elemental analysis calculated (%) for C₃₀H₃₆Cl₂N₂O₁₃Pt.H₂O: C 39.31, H 4.18, N 3.06; found: C 39.19, H 4.20, N 2.95. ¹⁹⁵Pt (DMSO-d₆, 107.6 MHz): δ PPM 1230.3.

Synthesis of PLGA-PEG-NH₂

PLGA-*b*-PEG-NH₂ was synthesized by using an amide coupling reaction. NH₂-PEG-NH₂ (1 g, 0.5 mmol), PLGA-COOH (0.975 g, 0.167 mmol), and 4-dimethylaminopyridine (20.3 mg, 0.167 mmol) in 20 mL dry CH₂Cl₂ were stirred at 0°C. DCC (103 mg, 0.5 mmol) in 3 mL dry CH₂Cl₂ was added drop wise to the solution. The solution was warmed to room temperature and stirred overnight. It was then filtered to remove the dicyclohexylurea byproduct, precipitated using a mixture of 50:50 methanol-diethyl ether, isolated via centrifugation (5000 rpm, 4 °C, 10 min), and lyophilized overnight. PLGA-*b*-PEG-NH₂ was isolated as a white solid. 38% yield (498 mg produced). ¹H NMR (CDCl₃, 400 MHz): δ ppm, 5.24 (m, 35H), 4.81 (m, 70H), 3.68 (s, 126H), 1.58 (m, 106H), ¹³C NMR (CDCl₃, 200 MHz): δ ppm 169.41, 169.29, 166.42, 166.33, 70.54, 69.17, 69.01, 60.80, 16.67, 16.63.

Synthesis of PLGA-PEG-TPP

(5-carboxypentyl)triphenylphosphonium (6-hexanoic TPP acid) (133mg, 0.294 mmol) and N-hydroxysuccinimide (NHS) (33.8mg, 0.294 mmol) were dissolved in 5 mL of CH₂Cl₂ and stirred at 0°C. DCC (60 mg, 0.294 mmol) was dissolved in 1 mL of CH₂Cl₂, added drop wise into the reaction mixture and stirred overnight at room temperature. DCU was filtered off, and the solution was evaporated. It was then redissolved with 10 mL of CH₂Cl₂ and PLGA-PEG-NH₂ (471 mg, 0.0589 mmol) and triethylamine (Et₃N) (8.3 μL) were added. The reaction was stirred overnight and reprecipitated with 10% methanol in diethyl ether 3 times and lyophilized. 59% yield (290 mg produced) ¹H NMR (CDCl₃, 400 MHz): δ ppm, 7.74 (m, 16H), 5.21 (m, 35H), 4.83 (m, 63H), 3.64 (s, 122H), 1.57 (m, 103H) ¹³C NMR (CDCl₃, 200 MHz): δ ppm 169.29, 166.33, 133.76, 133.66, 133.56, 130.54, 130.42, 70.54, 69.00, 60.80, 16.67

Nanoparticle Formation

PLGA-*b*-PEG-NH₂ or PLGA-*b*-PEG-TPP (50 mg mL⁻¹) and Platin-*C* (10 mg mL⁻¹) were dissolved in DMF. Solution containing different ratio of Platin-*C* and 5 mg mL⁻¹ of polymer were added drop wise into water with constant stirring at room temperature for 2 h. It was washed 3 times with nanopure water with Amicon ultracentrifugation filtration membranes with a molecular weight cutoff of 100 kDa (3000 rpm, 4°C). NPs were suspended in 1 mL of water.

The (3-(4,5-dimethylthiazol-2-yl)-2,5-diphenyltetrazolium bromide or MTT Assay and Data Analysis

The cytotoxic behaviors were evaluated using the MTT assay against PC3, DU145, LNCaP, MCF-7, A2780 CP70 and RAW 264.7 cells. Cells (2000 cells/well for PC3, and DU145 cells; 10000 cells/well for LNCaP and RAW 264.7) were seeded on a 96-well plate in 100 μ L of desired medium and incubated for 24 h. The cells were treated with different constructs at varying concentrations and incubated for 72 h at 37 °C except for RAW 264.7 macrophages. An incubation time period of 24 h was used for the macrophages. The cells were then treated with 20 μ L of MTT (5 mg/mL in PBS) for 5 h. The medium was removed, the cells were lysed with 100 μ L of DMSO, and the absorbance of the purple formazan was recorded at 550 nm using a Bio-Tek Synergy HT microplate reader. Each well was performed in triplicate. Cytotoxicity was expressed as a mean percentage increase relative to the unexposed control \pm SD. Control values were set at 0% cytotoxicity or 100% cell viability. Cytotoxicity data (where appropriate) was fitted to a sigmoidal curve and a three parameters logistic model used to calculate the IC₅₀, which is the concentration of chemotherapeutics causing 50% inhibition in comparison with untreated controls. The mean IC₅₀ is the concentration of agent that reduces cell growth by 50% under experimental conditions and is the average of at least four independent measurements that were

reproducible and statistically significant. The IC₅₀ values were reported at ±95% confidence intervals. This analysis was performed with GraphPad Prism (San Diego, U.S.A).

***In Vitro* COX Inhibition Assay**

An enzyme immunoassay (EIA) kit from Cayman Chemicals (catalogue number 560101) was used to assess the ability of Platin-A to inhibit ovine COX-1 and COX-2. The COX inhibition assay was performed as prescribed by the manufacturer's protocol. All stock solutions were prepared according to the manufacturer's instructions. This inhibition assay was performed by using a two-step process: COX reaction and EIA. The COX reaction involved preparation of the following samples.

(i) *Background samples*: COX-1 and COX-2 were inactivated by transferring 20 µL of each enzyme to an eppendorf tube and placing the tube in boiling water for 3 min. After inactivation, 970 µL of reaction buffer, 10 µL of heme, and 10 µL of inactive COX-1 or inactive COX-2 were added to the test tube.

(ii) *COX-1 or COX-2 100% initial activity samples*: 950 µL of reaction buffer, 10 µL of heme, 10 µL of COX-1 or COX-2, and 20 µL of reaction buffer were added to each test tube.

(iii) *COX-1 or COX-2 inhibitor samples*: 950 µL of reaction buffer, 10 µL of heme, 10 µL of COX-1 or COX-2 and 20 µL of the COX-1 and COX-2 inhibitors under investigation, and aspirin and Platin-A of different concentrations (0.25, 0.5, 0.75, 1, and 1.5 mM for COX-1; 0.75, 1, 1.25, 1.5, and 2 mM for COX-2) were added to each test tube.

All the samples were incubated for 5 min in a water bath at 37 °C. Reactions were initiated by adding 10 µL of arachidonic acid to all samples. These samples were vortexed and incubated for another 2 min in a water bath at 37 °C. 50 µL of 1 M HCl was added to each test tube to stop enzyme catalysis. The test tubes were removed from the water baths and 100 µL of saturated

stannous chloride solution was added to each test tube. This mixture was then vortexed. These samples were incubated for 5 min at room temperature. Background samples were diluted to 1:100 times, and the COX 100% initial activity and COX inhibitor samples were diluted to 1:2000 times.

For EIA, 100 μL of EIA buffer was added to non-specific binding wells and 50 μL of EIA buffer to maximum binding wells. 50 μL of PG screening standard was added to each standard well. 50 μL of background samples were added to the background sample wells. 50 μL of COX 100% initial activity samples were added to the specific wells. 50 μL of COX inhibitor samples and aspirin and Platin-A samples were added to the specific wells. 50 μL of PG screening acetylcholinesterase (AChE) tracer was added to all the wells except to the total activity and blank wells. 50 μL of PG screening EIA antiserum was added to all wells, except to the total activity, non-specific binding, and the blank wells. EIA plate was covered with plastic film and incubated for 18 h at room temperature on an orbital shaker. Wells were emptied and rinsed 5 times with a wash buffer. Ellman's reagent (200 μL) was added to each well followed by the addition of 5 μL of tracer to the total activity well. The EIA plate was again covered with plastic film and then incubated for 1 h at room temperature on an orbital shaker in the dark. Absorbance was recorded at a wavelength of 410 nm by using a plate reader.

Results and Discussions

***In vitro* cytotoxicity on prostate cancer cells**

High expressions of COX-2 are found in various cancers; however, contradictory results exist for PCa cell lines as well as for tissue.²⁹ Therefore, we tested the anti-proliferative properties of Platin-A on androgen-unresponsive PC3 and DU145 PCa cells that differ in their

malignant potentials. Platin-A demonstrated an IC₅₀ value comparable to that of cisplatin alone and to an equimolar mixture of cisplatin and aspirin in PC3 cells (Figure 3.1., Table 3.1.). Similar trends were observed in DU145 for Platin-A and cisplatin (Figure 3.1., Table 3.1.). Platin-A exhibited a slightly higher IC₅₀ value than an equimolar mixture of cisplatin and aspirin in DU145. However, in LNCaP cells, Platin-A was more active than in an equimolar mixture of cisplatin and aspirin. In general, Pt(IV) compounds are less cytotoxic compared with their active Pt(II) form. Comparable cytotoxicities of Platin-A, a Pt(IV) prodrug, with cisplatin demonstrated its unique anti-proliferative potency in PCa cells.

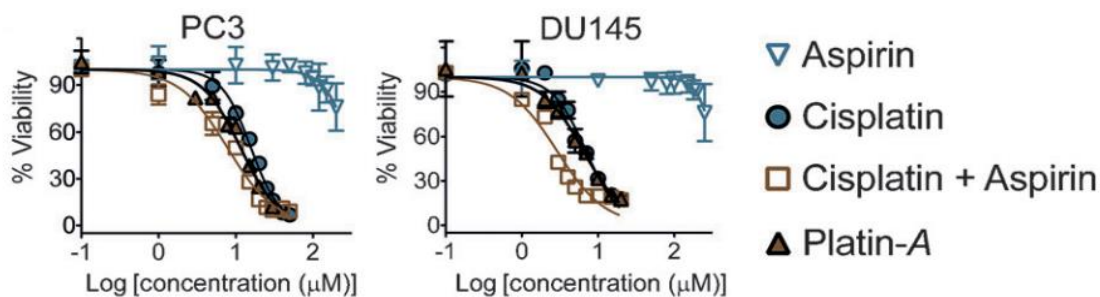


Figure 3.1. Cytotoxic profiles of Platin-A, cisplatin, and an equimolar mixture of cisplatin and aspirin in PCa cell lines.

Table 3.1. Comparison of IC₅₀ values of cisplatin, an equimolar mixture of cisplatin and aspirin, and Platin-A in different PCa cells.

IC ₅₀ (μM)	Platin-A	Cisplatin	Cisplatin + Aspirin
PC3	15 ± 5	14 ± 4	14 ± 6
DU145	8 ± 3	5 ± 2	4 ± 1

***In vitro* COX inhibitory properties of Platin-A**

In vitro COX inhibitory properties of Platin-A were studied using an enzyme immunoassay (EIA). Platin-A showed a similar inhibition of both COX-1 and COX-2 as shown by aspirin in a concentration independent manner (Figure 3.2.). Aspirin is known to be more potent than salicylate as an inhibitor of COX-1 or COX-2³⁰. These remarkable COX inhibitory properties of Platin-A indicated its potential in reducing tumor-associated inflammation.

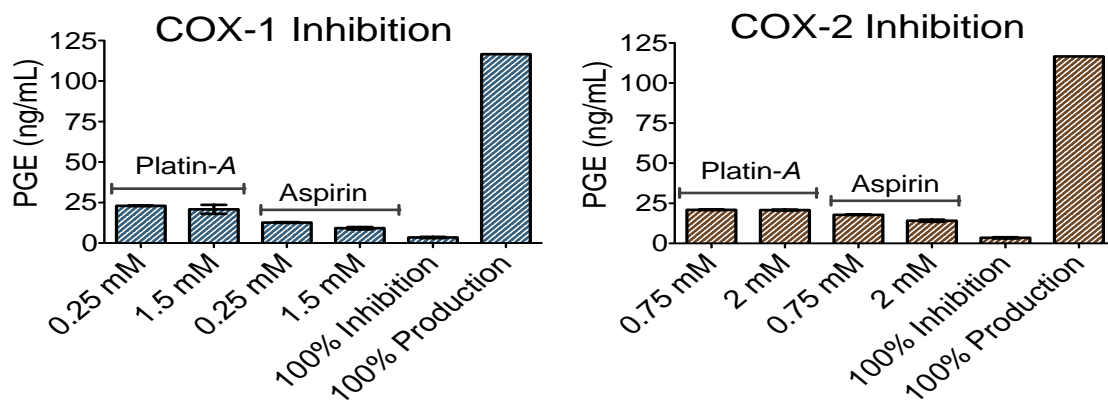


Figure 3.2. Inhibition of ovine COX-1 and COX-2 by Platin-A.

Limitations of Platin-A

Platin-A displays similar anti-cancer effect to cisplatin on different prostate cancer cell lines. Also, it reduces the inflammation by down-regulating COX-2 level, proinflammatory cytokines, IL-6 and TNF- α , and up-regulating anti-inflammatory cytokine, IL-10. With significant properties of Platin-A, assumption is made that encapsulation of compound into polymeric NPs would further enhance its properties. However, because of its water solubility, encapsulation efficiency was low to encapsulate in NPs. Therefore, use of different anti-inflammatory compound with cisplatin was investigated.

Synthesis and Characterization of Pt(IV)(curcumin)₂

In Pt(IV)(curcumin)₂, curcumin moiety was introduced to cisplatin by a reaction of *c,c,t*-[Pt(NH₃)₂Cl₂(OH)₂] with curcumin anhydride. Figure 3.3. represents a schematic diagram of the synthesis of Pt(IV)(curcumin)₂.

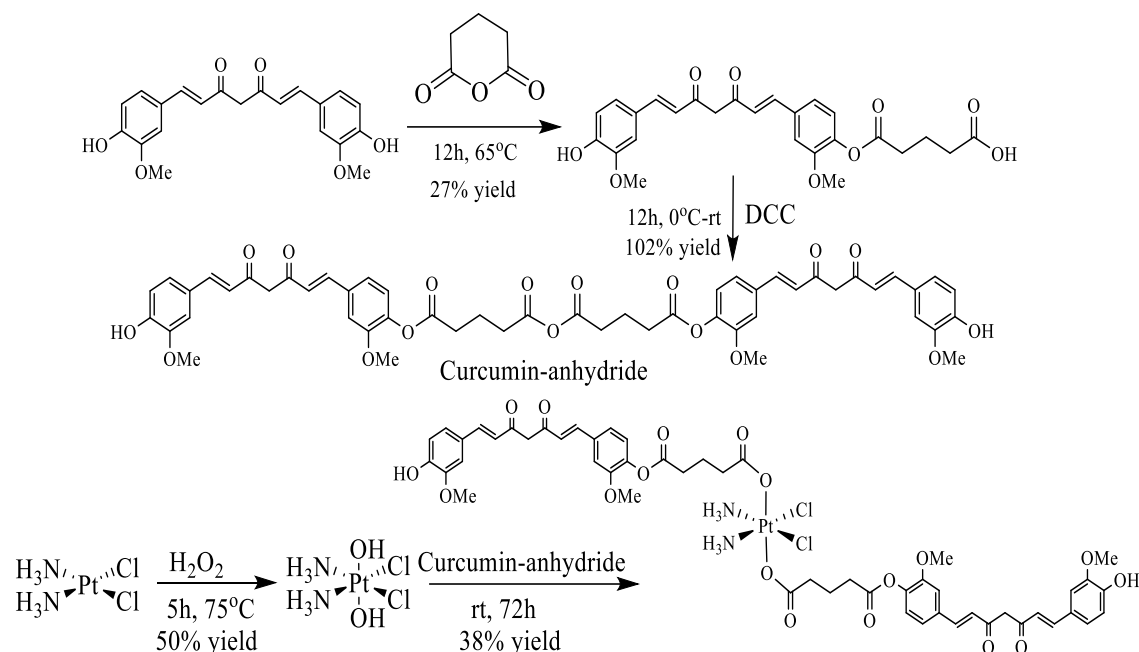


Figure 3.3. Schematic diagram of synthesis of Pt(IV)(curcumin)₂.

Pt(IV)(curcumin)₂ was characterized by using ¹H NMR, ¹³C NMR, and ¹⁹⁵Pt NMR. Analytical instruments, high resolution mass spectrometry (HRMS) and high performance liquid chromatography (HPLC) were also used to verify the dicurcumin Pt(IV). Characterizations of Pt(IV)(curcumin)₂ are shown in figure 3.4., figure 3.5, figure 3.6, figure 3.7, figure 3.8, and figure 3.9. Presence of ¹H NMR peak at 6.5, NH₃ peak, shows an attachment on both hydroxyl group from dihydroxy Pt(IV). Also, isotopic pattern from HRMS and single peak at HPLC

represents Pt(IV)(curcumin)₂. However, there are two peaks shown on ¹⁹⁵Pt NMR, monocurcumino Pt(IV) and Pt(IV)(curcumin)₂.

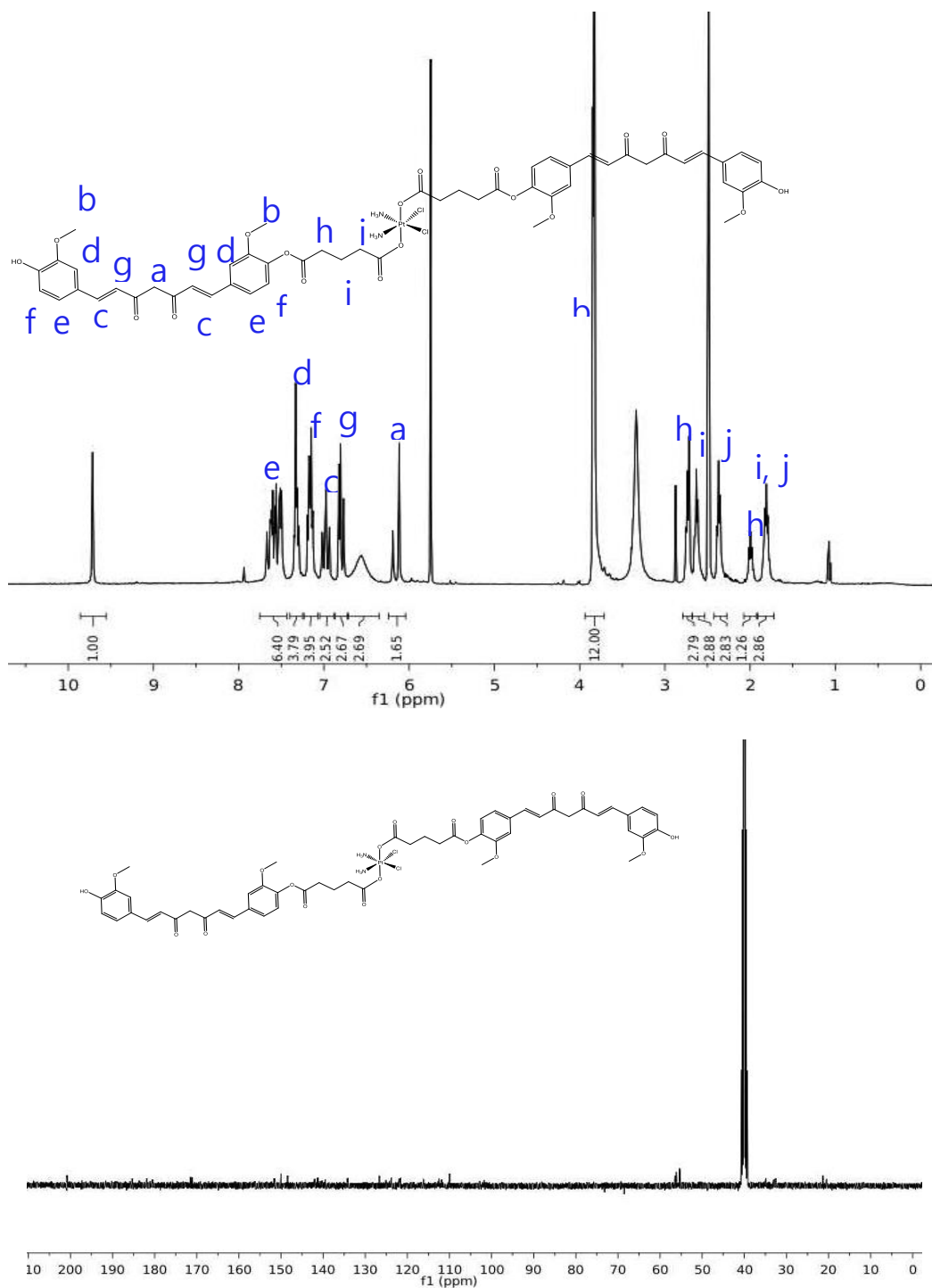
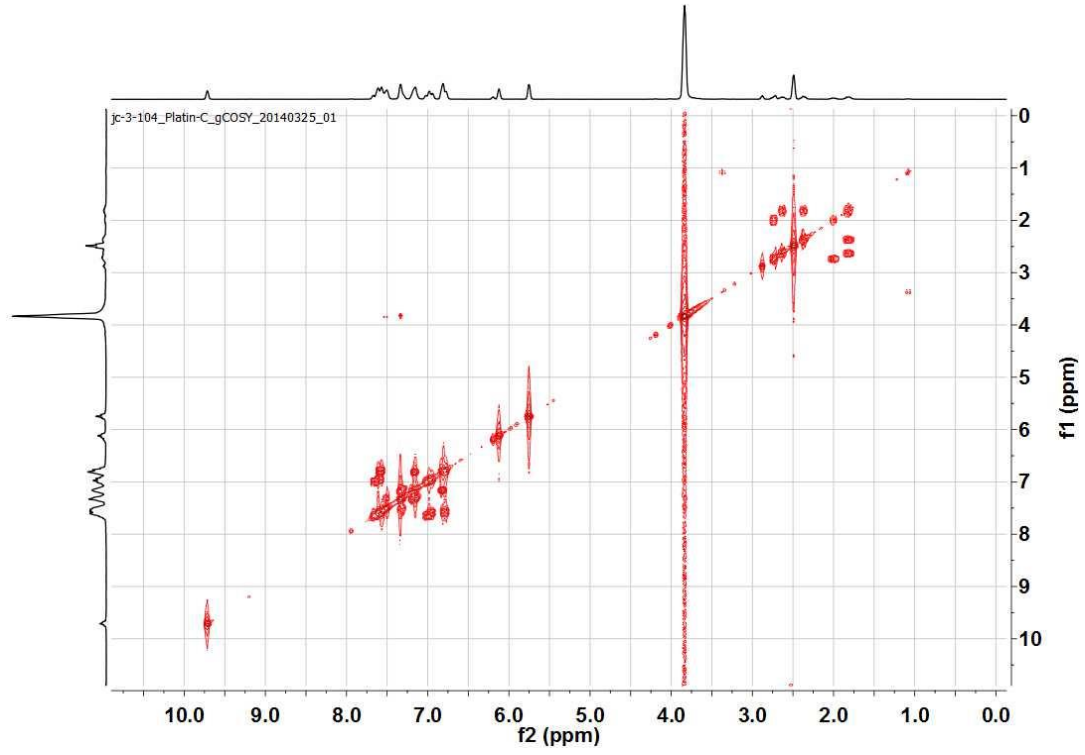


Figure 3.4 ¹H NMR, ¹³C NMR of Pt(IV)(curcumin)₂ in DMSO-d₆.



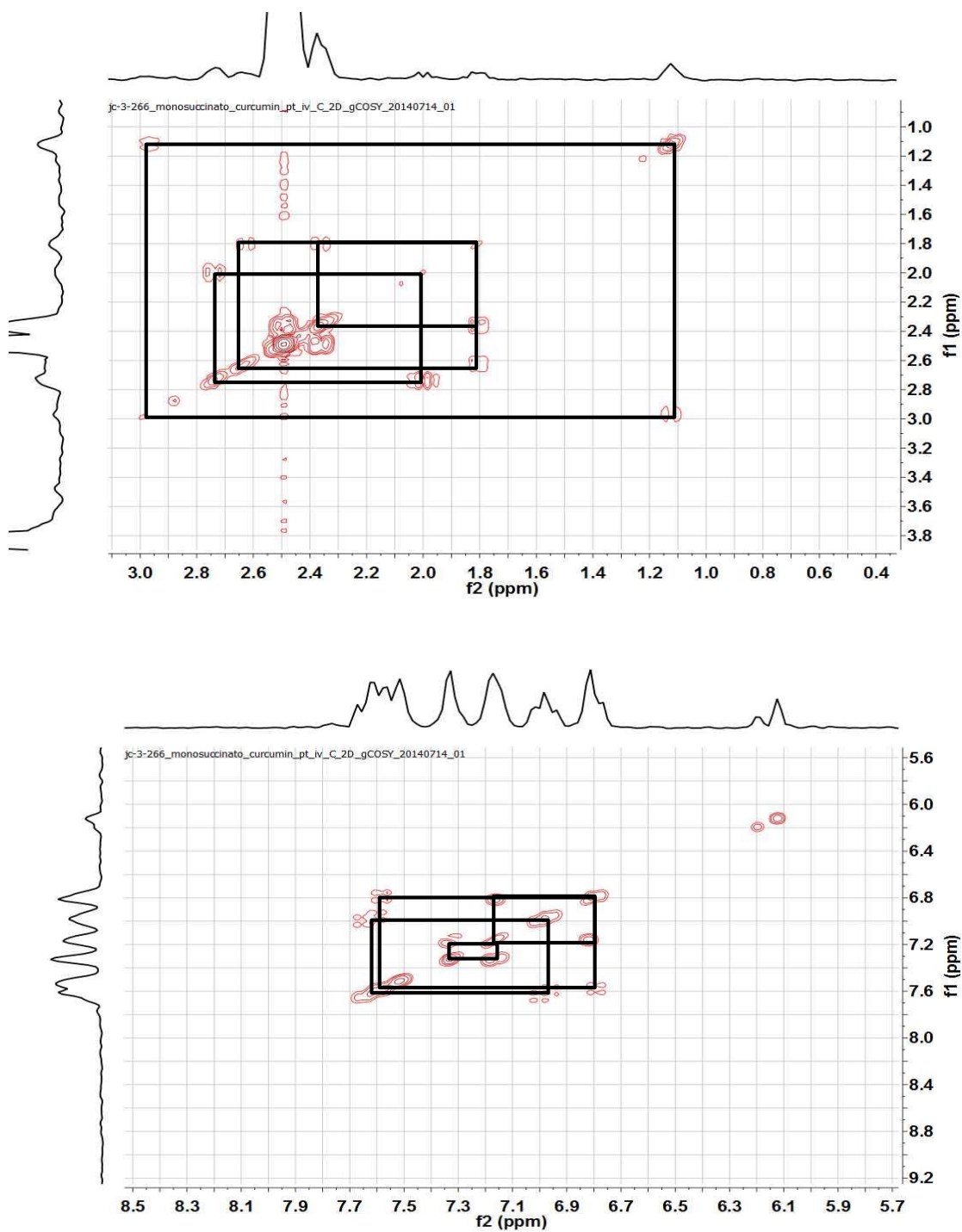


Figure 3.5. Full and extended spectrum of 2D NMR of Pt(IV)(curcumin)₂ in DMSO-d₆.

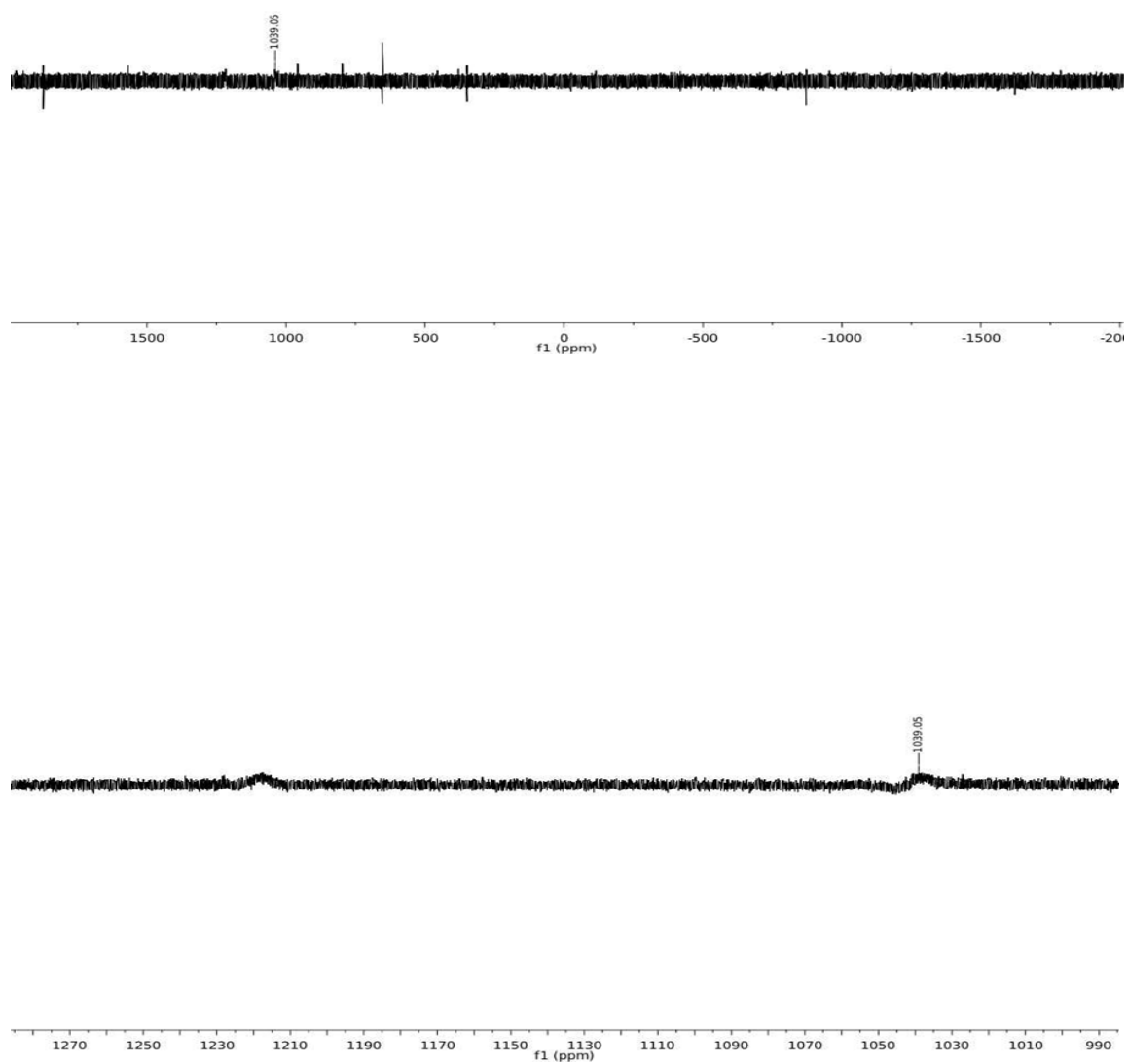


Figure 3.6. Full spectrum (top) and positive spectrum (bottom) ^{195}Pt NMR of $\text{Pt(IV)(curcumin)}_2$ in DMSO-d_6 .

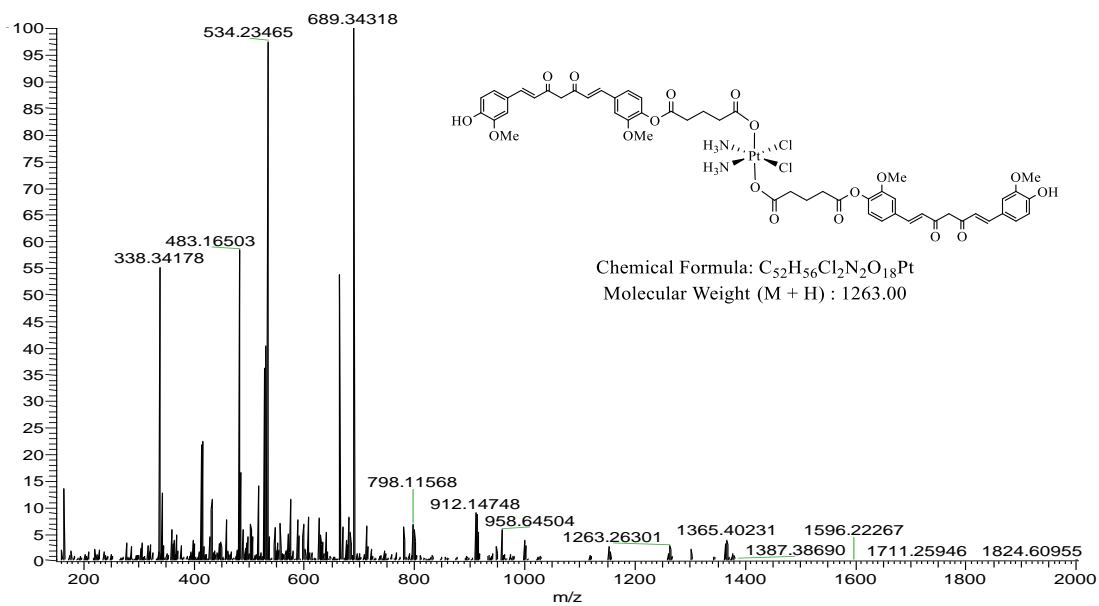
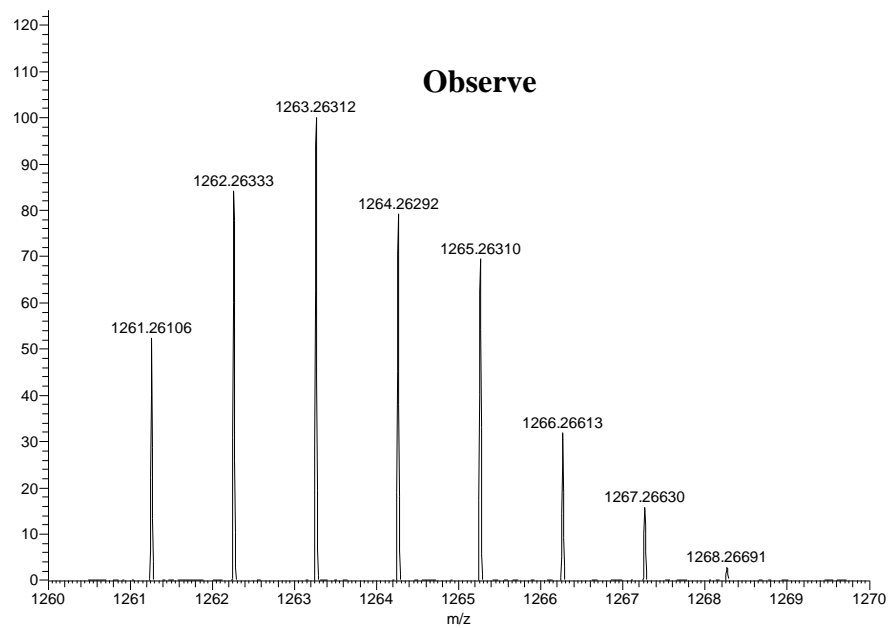


Figure 3.7. Positive ion ESI-HRMS spectrum of Pt(IV)(curcumin)₂.



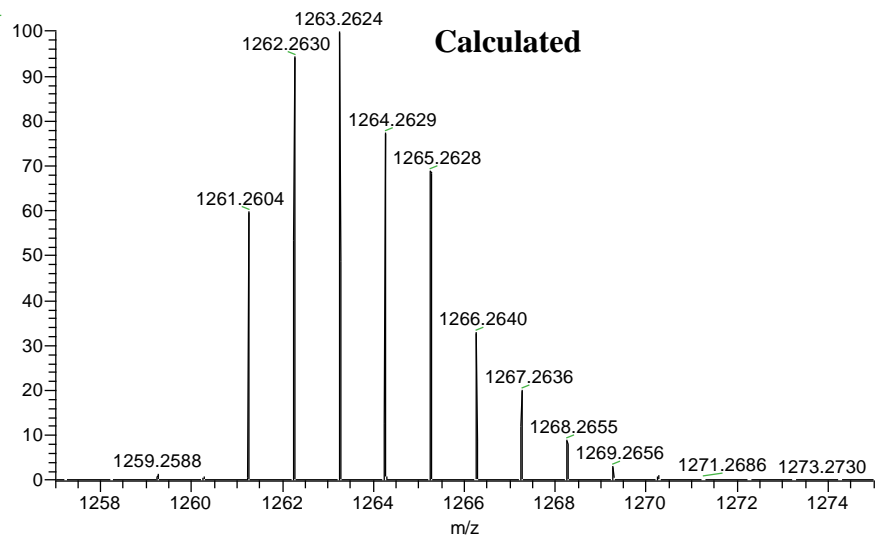


Figure 3.8. Observed (top) and calculated (bottom) isotopic peak pattern analysis of Positive ion ESI-HRMS spectrum of Pt(IV)(curcumin)₂.

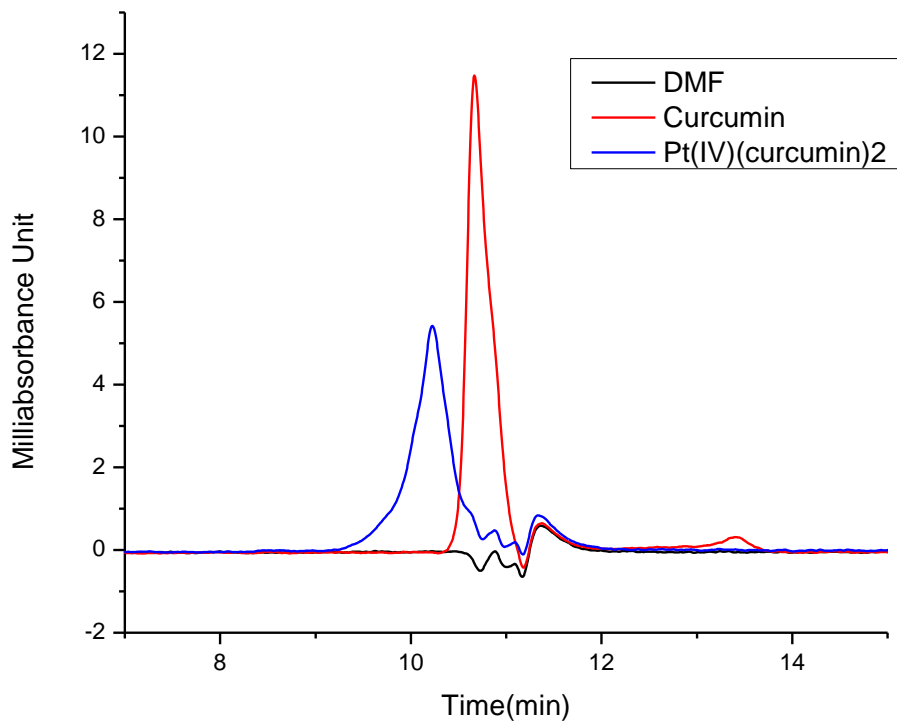


Figure 3.9. HPLC analysis of Pt(IV)(curcumin)₂ and curcumin.

Drawback of Pt(IV)(curcumin)₂

Pt(IV)(curcumin)₂ has a major problem of having both mono- and di-curcumin products. Increasing the reaction time, equivalent ratio, and decreasing the volume of solvent were not able to solve the problem. Moreover, owing to the similarities in solubilities between mono- and di-curcumin products, it was difficult to purify the desired product, hence the design strategy was modified to synthesize Platin-C.

Synthesis of Platin-C

In Platin-C, curcumin moiety was introduced to cisplatin by a reaction of monosuccinato Pt(IV) with curcumin anhydride. Figure 3.10. represents a schematic diagram of the synthesis of Platin-C. Platin-C was characterized using several spectroscopic and analytical techniques (figure 3.11-15). Like dicurcumino Pt(IV), Peak at 6.5 represents curcumin and succinic acid conjugation to cisplatin and unlike dicurcumino Pt(IV), ¹⁹⁵Pt NMR expresses only one peak at positive spectrum which shows only one product. Also, isotopic pattern from HRMS and single peak at HPLC confirms it. Additionally, elemental analysis represents similar carbon, hydrogen, and nitrogen percent of Platin-C.

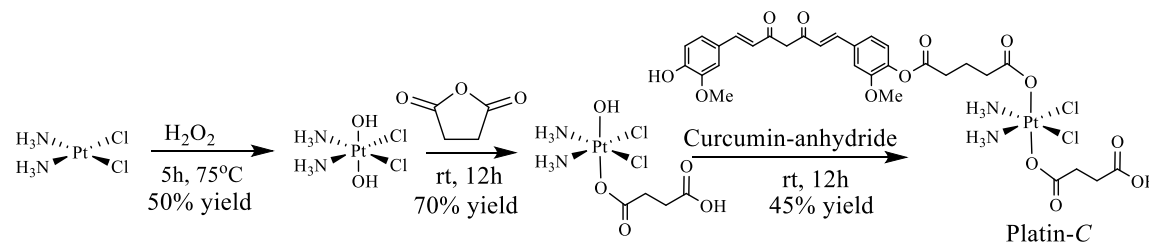


Figure 3.10. Schematic diagram of synthesis of Platin-C

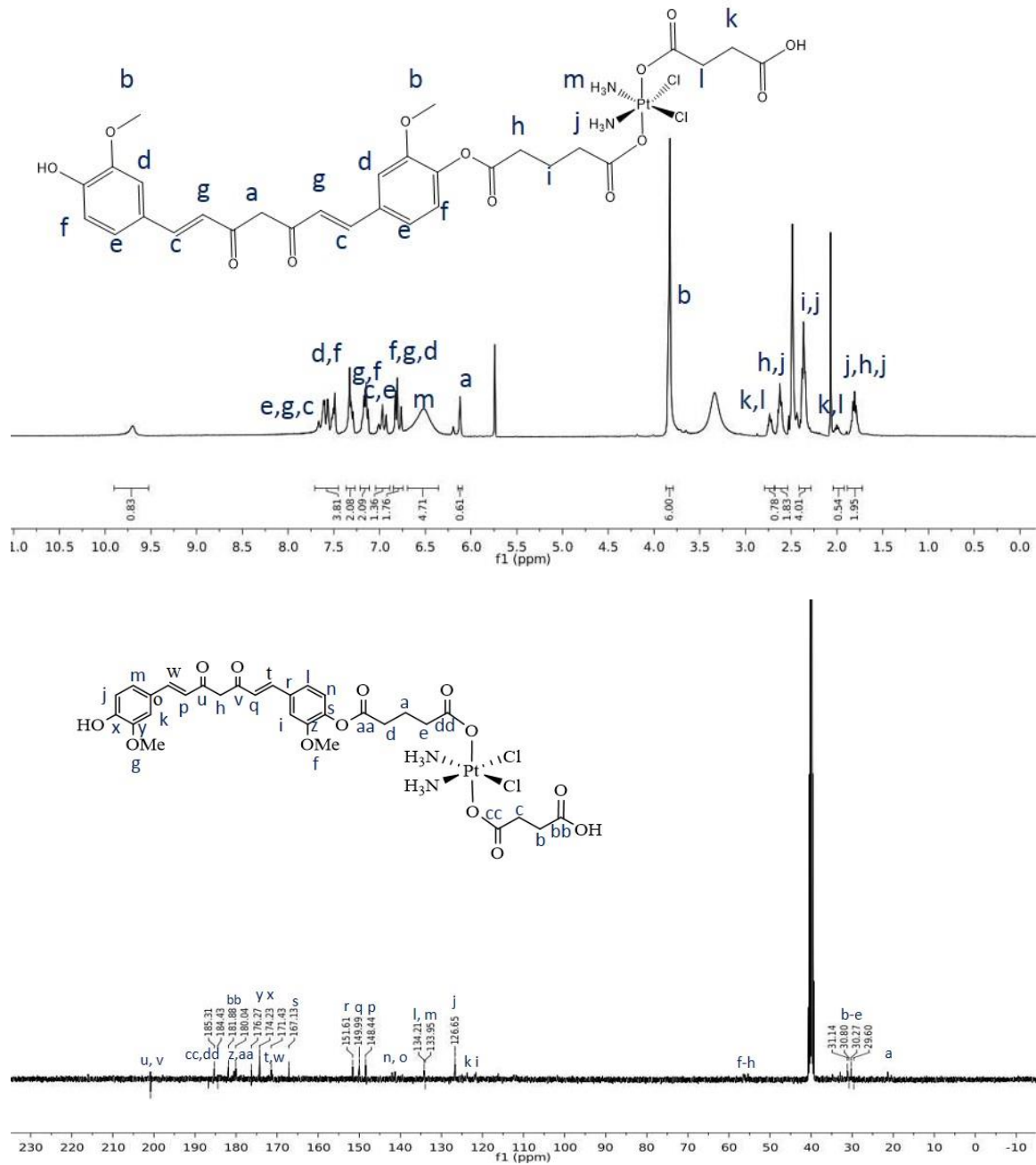


Figure 3.11 ¹H NMR, ¹³C NMR of Platin-C in DMSO-d₆.

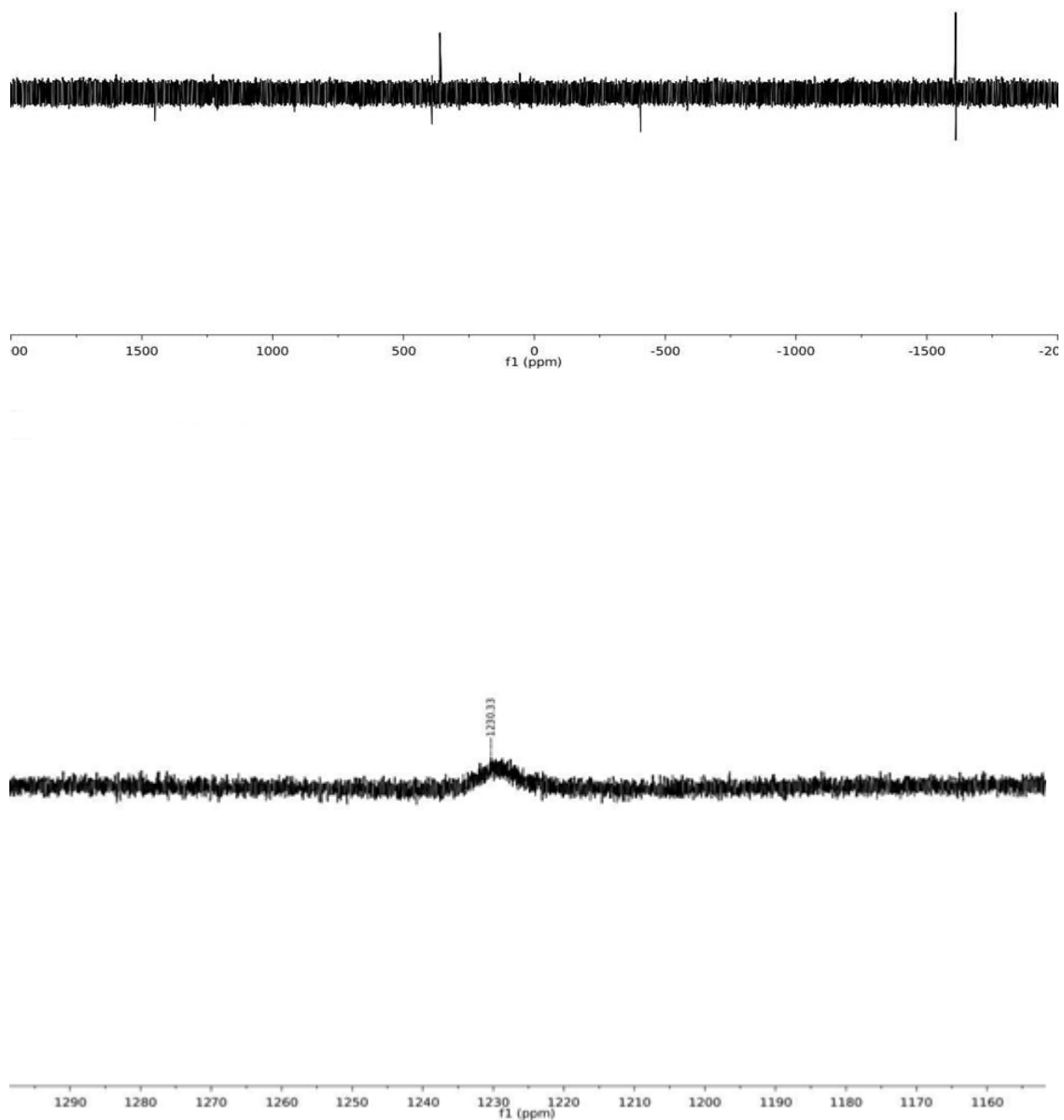


Figure 3.12. Full spectrum (top) and positive spectrum (bottom) ^{195}Pt NMR of Platin-C in DMSO-d_6

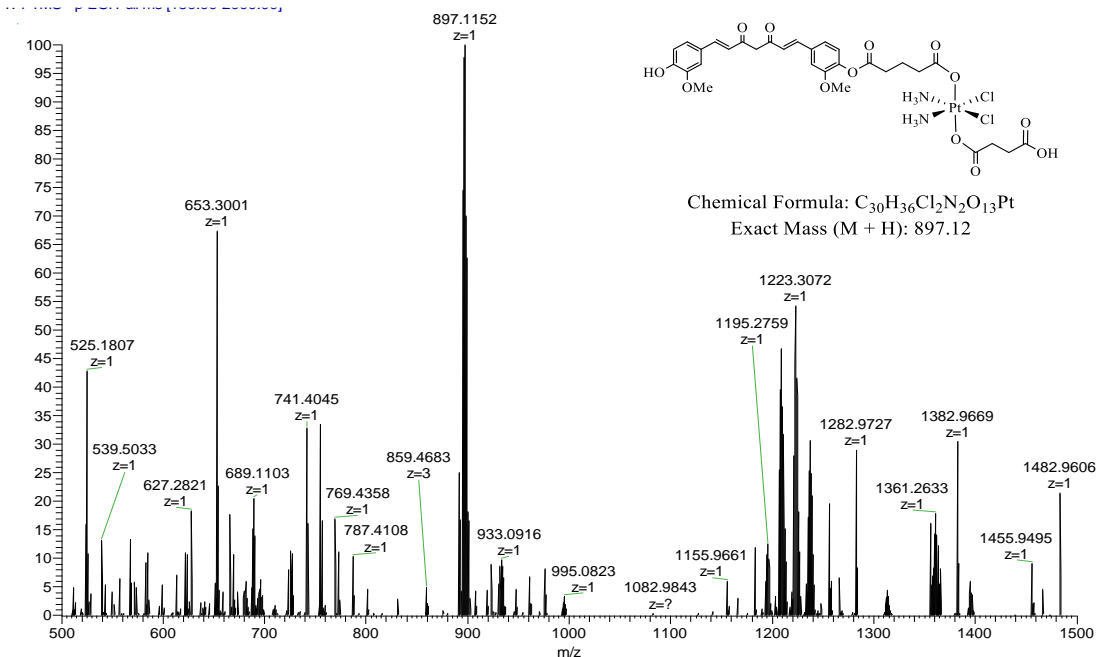
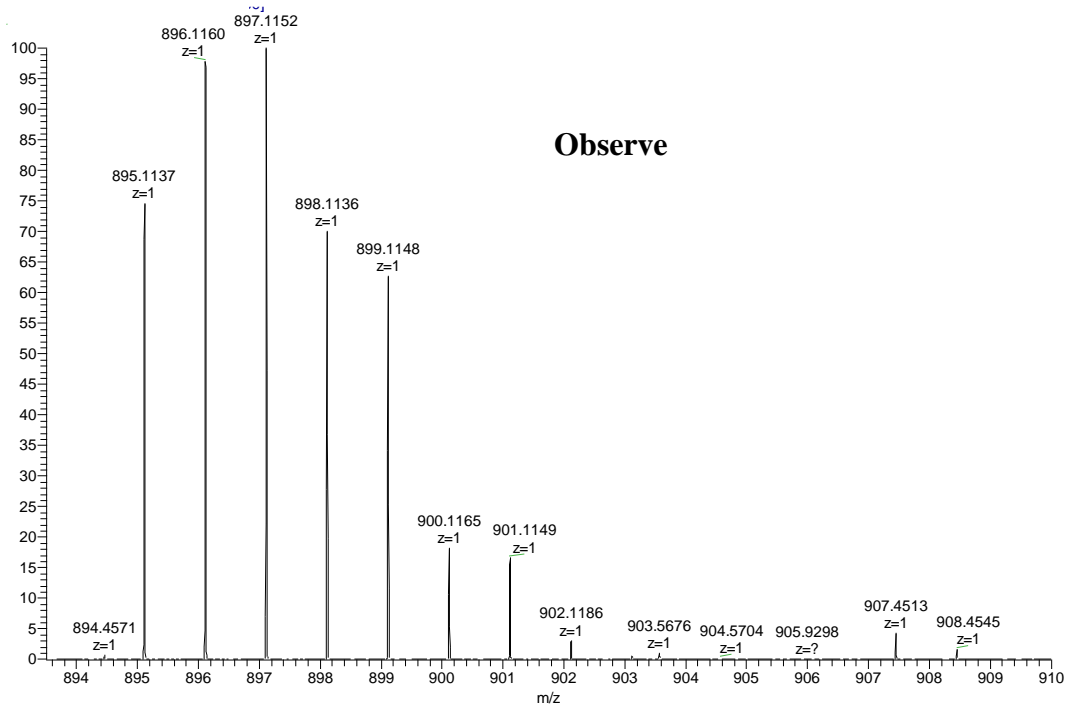


Figure 3.13. Positive ion ESI-HRMS spectrum of Platin-C.



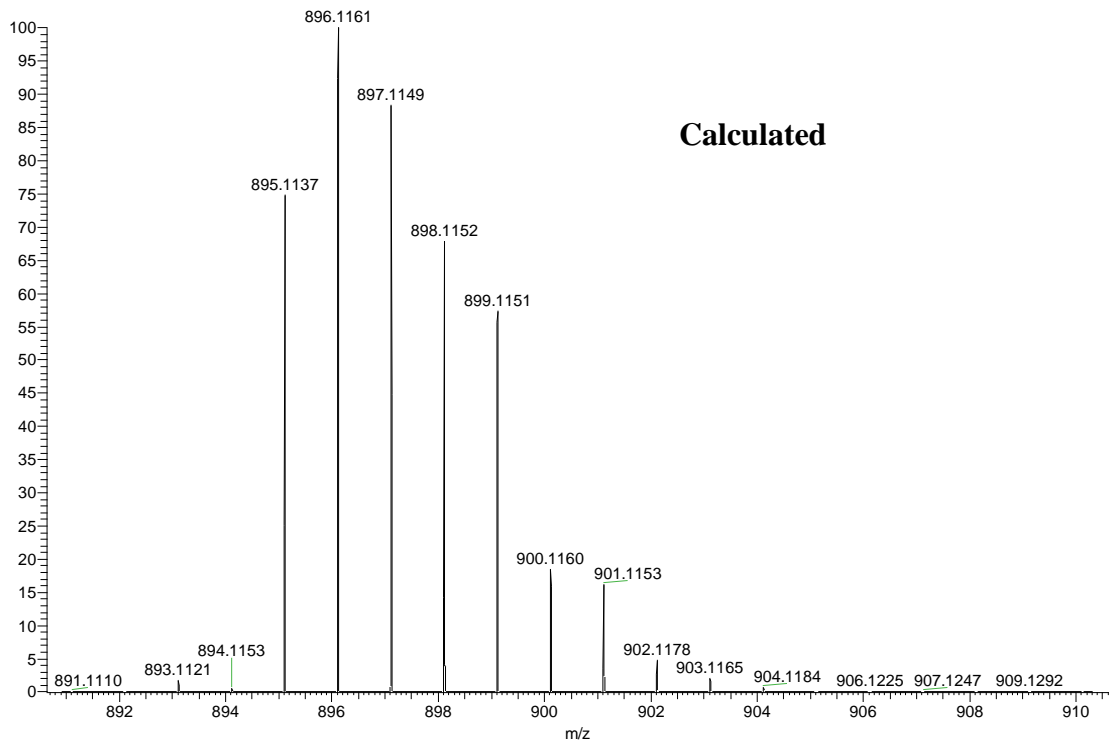


Figure 3.14. Observed (top) and calculated (bottom) isotopic peak pattern analysis of Positive ion ESI-HRMS spectrum of Platin-C.

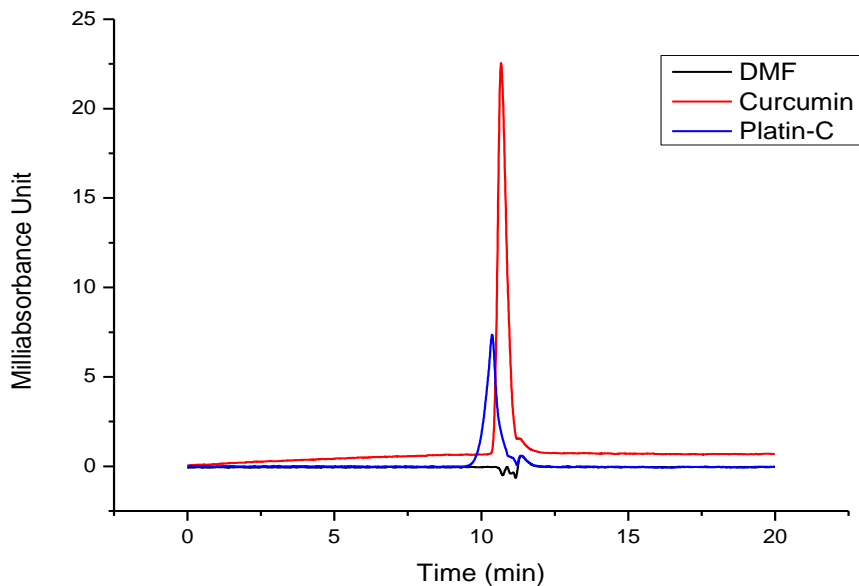


Figure 3.15. HPLC analysis of Platin-C and curcumin.

Synthesis of Polymer and Characterization of NPs

PLGA and PEG are both FDA-approved polymers, but have different properties- PLGA is hydrophobic, but PEG is hydrophilic. PLGA with carboxylic acid functionality (PLGA-COOH) and PEG with diamine (NH₂-PEG-NH₂) were conjugated via DMAP/DCC coupling as a non-targeted polymer. Further, PLGA-PEG-NH₂ was conjugated with (5-carboxypentyl)triphenylphosphonium via NHS/DCC coupling to place the targeting moiety, TPP, on the surface of the polymers. NT and T NPs were made by the nanoprecipitation method, self-assembly of NPs by hydrophilicity of a polymer. Polymers and Platin-C were dissolved in a water miscible solvent, DMF, and added drop wise into an aqueous solution to form self-assembled NPs. Because of the hydrophobic property of Platin-C, it embedded in the core of the NPs with PLGA, but PEG which is hydrophilic stretches out on the surface of NPs to increase the circulation period. Figure 3.16. represents a schematic diagram of the synthesis of polymers and the formation of NPs. Figure 3.17. represents ¹H and ¹³C NMR of T polymers and figure 3.18. shows GPC of different polymers and its molecular weights (Table 3.2.).

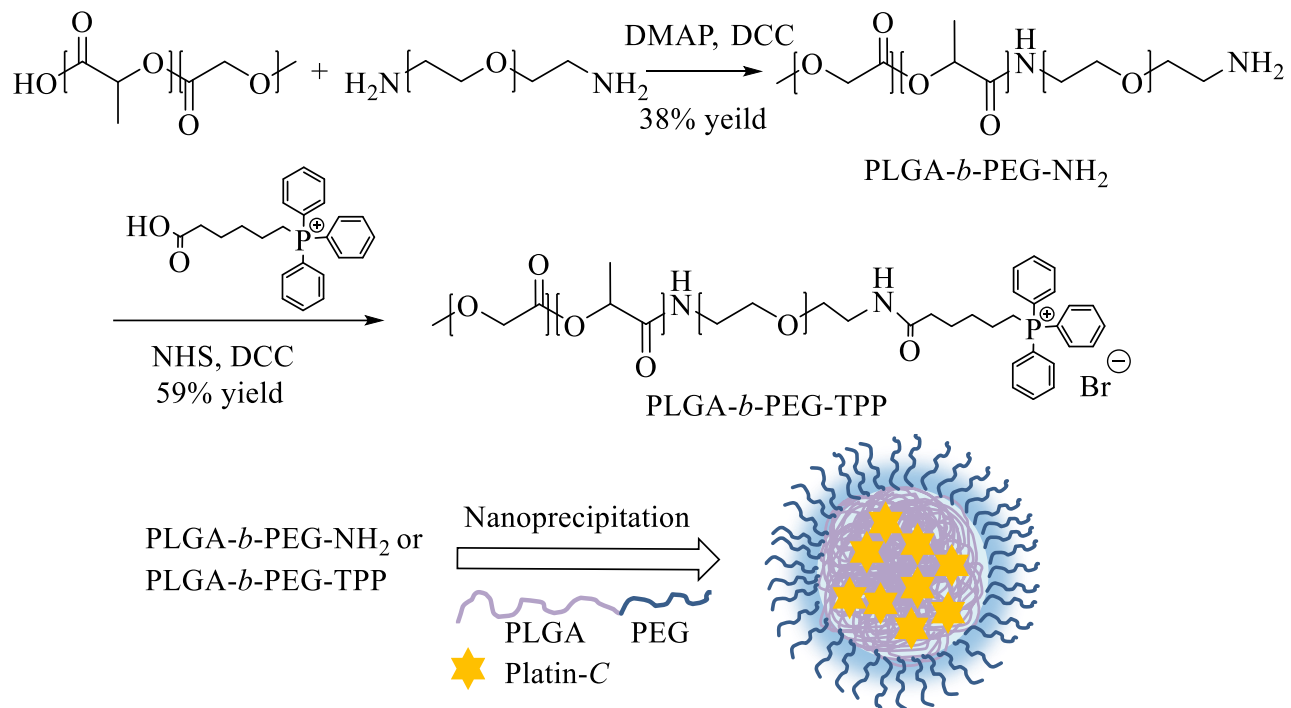


Figure 3.16. Schematic diagram of synthesis of non targeted and targeted Polymers and Formation of NPs.

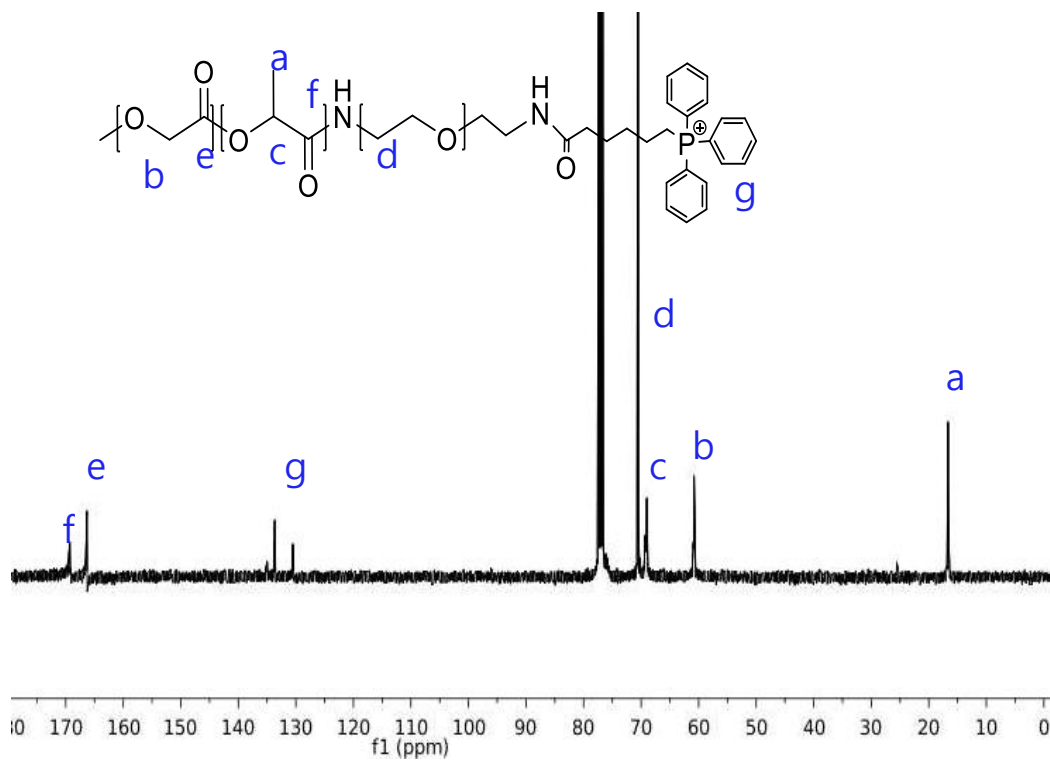
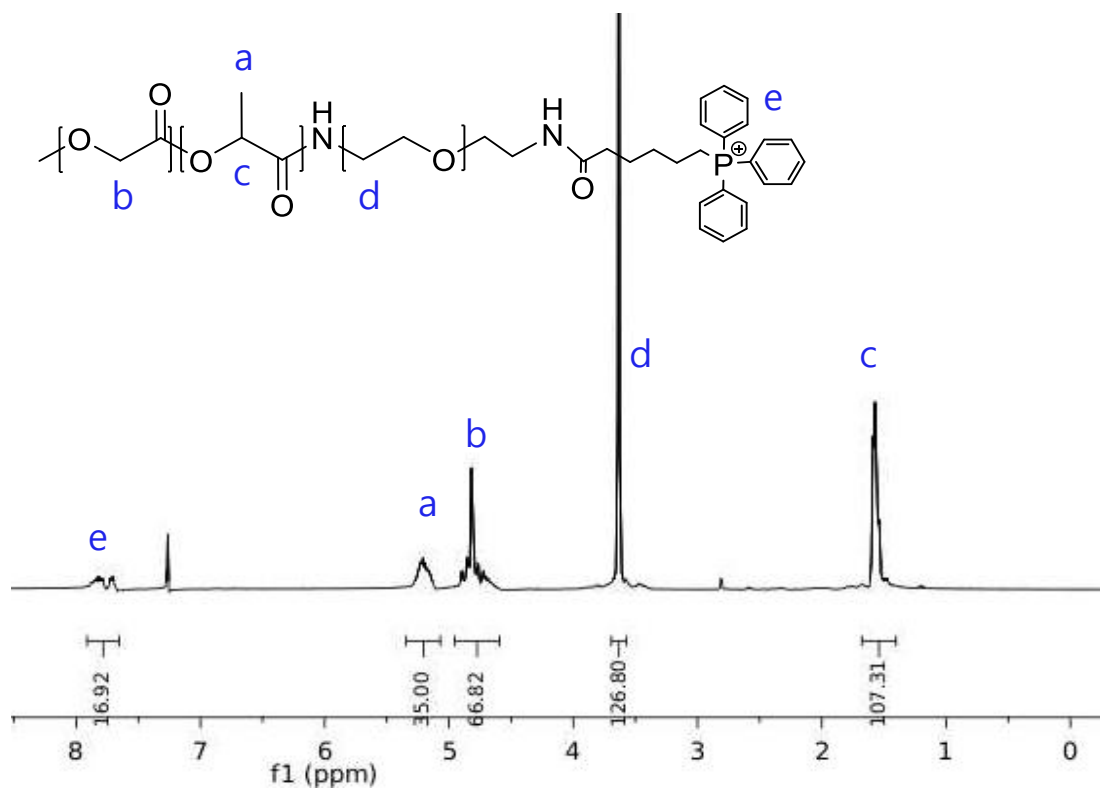


Figure 3.17. ^1H and ^{13}C NMR of PLGA-PEG-TPP (Targeted polymer).

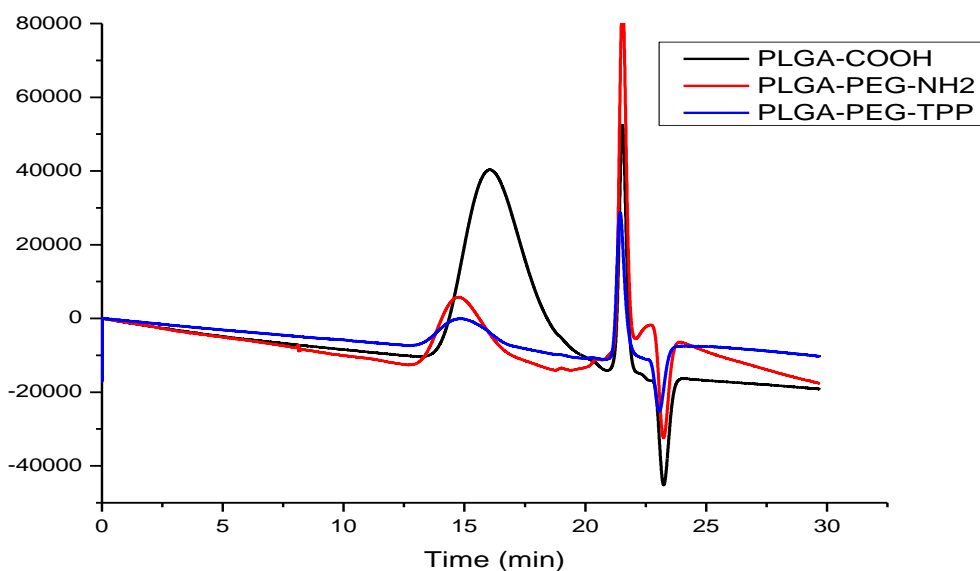


Figure 3.18. GPC of different Polymers.

Table 3.2. Comparison of molecular weights of PLGA-COOH, PLGA-*b*-PEG-NH₂, and PLGA-*b*-PEG-TPP as determined from gel permeation chromatographic (GPC) with THF

Molecular Weight	PLGA-COOH	PLGA- <i>b</i> -PEG-NH ₂	PLGA- <i>b</i> -PEG-TPP
M _w	8,227 g/mol	16,644 g/mol	16,905 g/mol
M _n	4,849 g/mol	11,574 g/mol	13,183 g/mol
PDI	1.69	1.44	1.28

Hydrodynamic diameter, zeta potential, and PDI were measured by DLS. To optimize the size and loading, multiple NPs were prepared by varying the weight percentage of Platin-C to polymer (% w/w) which represents in figure 3.19. The presence of a yellow color without precipitation in an aqueous solution implies that Platin-C embedded in NPs that confirmed the formation of NPs. Size of NPs were constant at 40 nm until 20% feed for both NT and T NPs.

After, size were started to increase. 40% and 50% of T NPs were not tested since it was not able to filter it with 0.2 μm syringe filter due to the size of the NPs so that it yields clear aqueous solution after filtration. Zeta potential for all NPs were positive that confirms that PEG which is conjugated to TPP moiety and NH_2 stretches out. Both NT and T empty NPs were showing zeta potential of 50 mV which dropped down to around 25 nm once Platin-C was encapsulated. Percent loading efficiency (% Loading), $\text{Platin-C in NPs} / \text{total polymer} * 100$ and percent encapsulation efficiency (% EE), $\text{Platin-C in NPs} / \text{total Platin-C in formulation} * 100$ were calculated to discover the optimum NP formulation, showing best % EE and % loading. In both NT and T NPs, 20% Platin-C formulation exhibited the best % loading and % EE, 5.6% and 28.0% for NT and 6.5% and 32.4% respectively. After the characterization of NPs, 20% Platin-C formulation was used for *in vitro* studies on both NT and T NPs. Figure 3.20. represents the % loading and % EE of NT and T NPs and figure 3.21 shows TEM image of Platin-C encapsulated NT and T NPs.

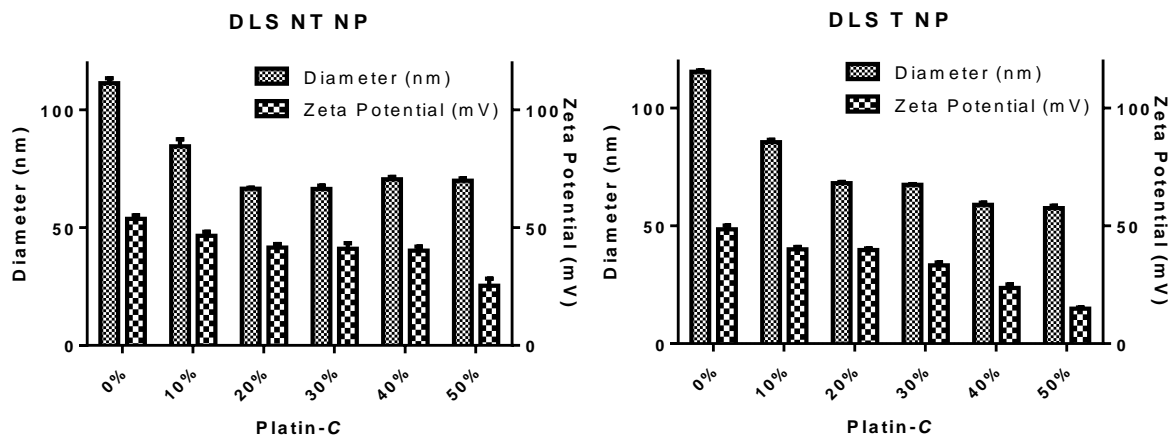


Figure. 3.19. Diameter and Zeta Potential of Different Weight Percentage of Platin-C NPs.

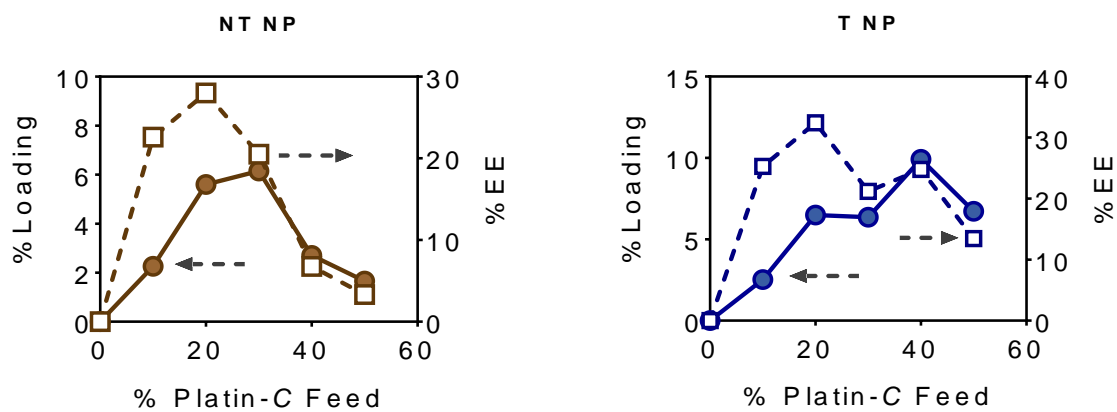


Figure 3.20. % Loading Efficiency and % Encapsulation Efficiency of NPs.

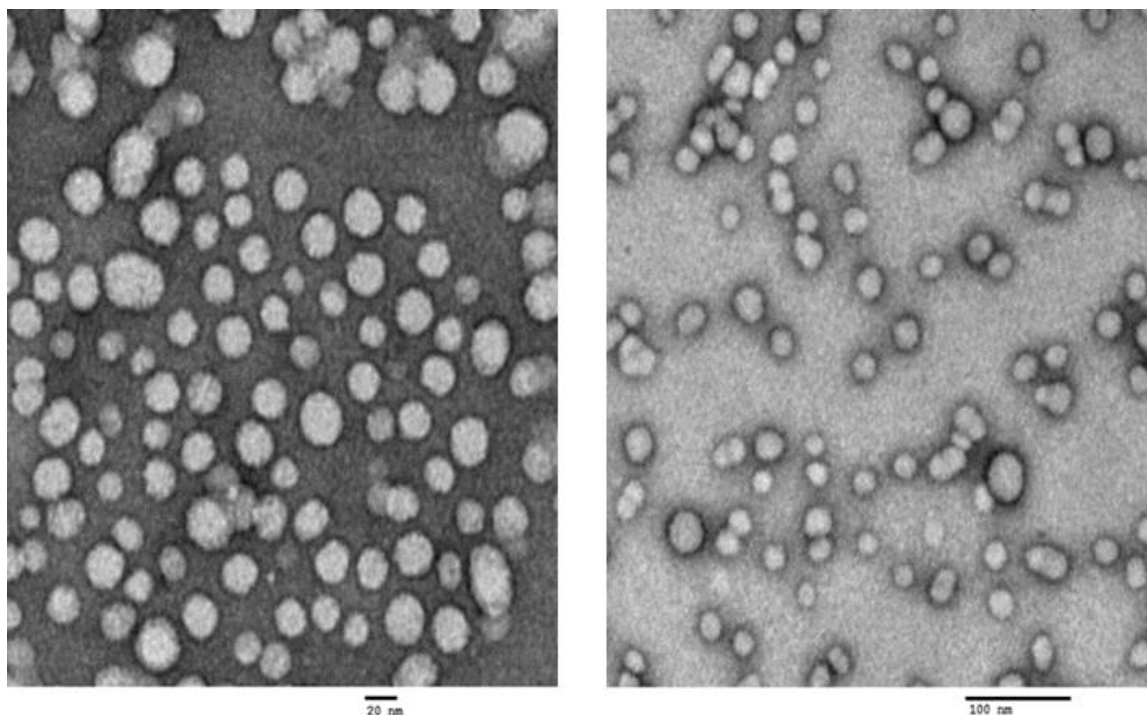


Figure 3.21. TEM of 20% Platin-C NT (left) and T (right) NPs.

***In vitro* cytotoxicity on different cells**

We tested the anti-proliferative properties of Platin-C on different cancer cell lines, A2780/CP70, MCF-7, and DU145. Platin-C demonstrated an IC_{50} value higher to that of cisplatin, curcumin alone, and to an equimolar mixture of cisplatin and curcumin (Figure 3.22., Table 3.3.). Similar trends were observed in DU145 and LNCaP cells for Platin-C and cisplatin (Figure 3.22., Table 3.3.). However, once it is encapsulated into NPs, IC_{50} values were slightly higher or comparable to cisplatin, curcumin alone. In general, Pt(IV) compounds are less cytotoxic compared with their active Pt(II) form since it is kinetically inert than Pt(II) compounds³¹. Comparable cytotoxicities of Platin-C NPs, demonstrated its unique anti-proliferative potency in cancer cells.

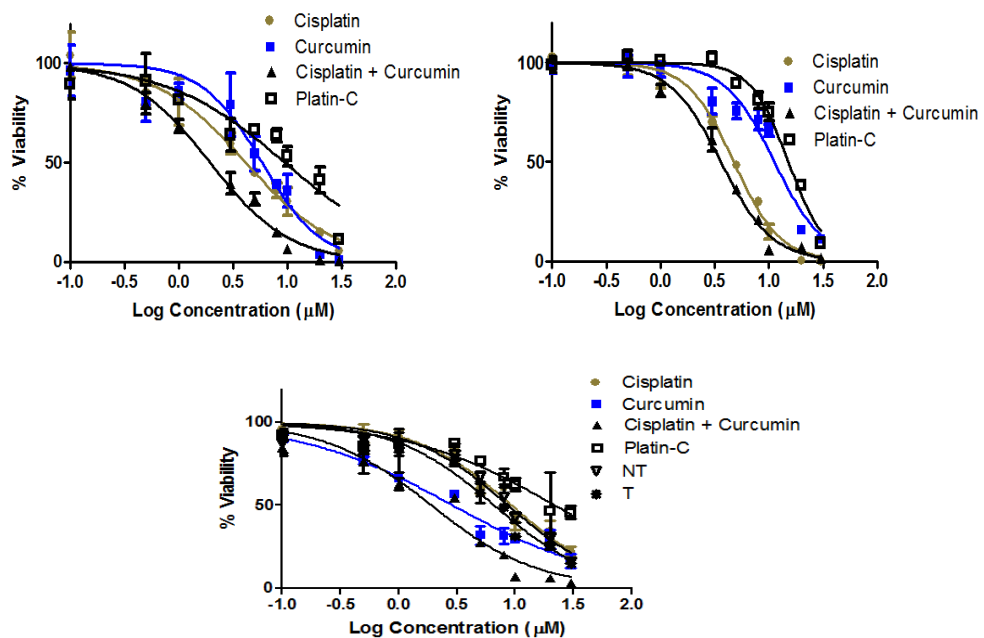


Figure. 3.22. Cytotoxic profiles of Platin-C NPs, free form of Platin-C, cisplatin, curcumin and an equimolar mixture of cisplatin and curcumin in A2780/CP70(top left), MCF-7(top right), and DU145(bottom) cell lines.

Table 3.3. Comparison of IC₅₀ values of Platin-C NPs, free form of Platin-C, cisplatin, curcumin and an equimolar mixture of cisplatin and curcumin in A2780 CP70(top left), MCF-7(top right), and DU145(bottom) cell lines.

IC ₅₀ (μM)	Cisplatin	Curcumin	Cisplatin + Curcumin	Platin-C	Platin-C NT NP	Platin-C T NP
	A2780/CP70	4.2	5.8	1.9	9.5	
MCF-7	4.7	11.2	3.6	15.1		
DU145	9.3	2.9	1.9	21.8	8.7	6.6

Conclusions

In summary, the unique chemo-anti-inflammatory molecule Platin-A, a prodrug for cisplatin and aspirin, was synthesized and characterized. A favorable reduction pattern of Platin-A was observed with the release of the biologically active platinum (II) form with concurrent liberation of aspirin. Platin-A showed cytotoxicity profiles comparable to cisplatin and demonstrated unique apoptosis-inducing potency in PCa cells. This work highlights the opportunities to uniquely combine NSAIDs, such as aspirin, with a cisplatin treatment regimen in the form of a single prodrug to increase efficiency and reduce side effects such as the ototoxicity of chemotherapy. Also, Platin-C, a prodrug of cisplatin and curcumin, was synthesized and characterized. Moreover, Platin-C was encapsulated with polymer PLGA-PEG-TPP for T NPs and with PLGA-PEG-NH₂ for NT NPs. These polymers provide a hydrophobic core for effective loading of Platin-C.

References

1. De Marzo, A. M.; Platz, E. A.; Sutcliffe, S.; Xu, J.; Grönberg, H.; Drake, C. G.; Nakai, Y.; Isaacs, W. B.; Nelson, W. G., Inflammation in prostate carcinogenesis. *Nat. Rev. Cancer* **2007**, *7* (4), 256-269.
2. Balkwill, F.; Mantovani, A., Inflammation and cancer: back to Virchow? *The lancet* **2001**, *357* (9255), 539-545.
3. Mauro, C.; Leow, S. C.; Anso, E.; Rocha, S.; Thotakura, A. K.; Tornatore, L.; Moretti, M.; De Smaele, E.; Beg, A. A.; Tergaonkar, V., NF-[kappa] B controls energy homeostasis and metabolic adaptation by upregulating mitochondrial respiration. *Nat. Cell Biol.* **2011**, *13* (10), 1272-1279.
4. Wu, M.; Lee, H.; Bellas, R. E.; Schauer, S. L.; Arsura, M.; Katz, D.; FitzGerald, M. J.; Rothstein, T. L.; Sherr, D. H.; Sonenshein, G. E., Inhibition of NF-kappaB/Rel induces apoptosis of murine B cells. *The EMBO J.* **1996**, *15* (17), 4682.
5. Beg, A. A.; Baltimore, D., An essential role for NF-kB in preventing TNF- α -induced cell death. *Science* **1996**, *274* (5288), 782-784.
6. Wang, C.-Y.; Mayo, M. W.; Baldwin, A. S., TNF-and cancer therapy-induced apoptosis: potentiation by inhibition of NF-kB. *Science* **1996**, *274* (5288), 784-787.
7. Van Antwerp, D. J.; Martin, S. J.; Kafri, T.; Green, D. R.; Verma, I. M., Suppression of TNF- α -induced apoptosis by NF-kB. *Science* **1996**, *274* (5288), 787-789.
8. Jamieson, E. R.; Lippard, S. J., Structure, recognition, and processing of cisplatin-DNA adducts. *Chem. Rev.* **1999**, *99* (9), 2467-2498.
9. Dhar, S.; Lippard, S.; Alessio, E., *Bioinorganic Medicinal Chemistry*. Wiley-VCH Weinheim, Germany: 2011; pp 79-95.

10. Prestayko, A.; d'Aoust, J.; Issell, B.; Crooke, S., Cisplatin (cis-diamminedichloroplatinum II). *Cancer treatment reviews* **1979**, *6* (1), 17-39.
11. Daugaard, G.; Abildgaard, U., Cisplatin nephrotoxicity. *Cancer chemoth. Pharm.* **1989**, *25* (1), 1-9.
12. Cvitkovic, E., Cumulative toxicities from cisplatin therapy and current cytoprotective measures. *Cancer Treat. Rev.* **1998**, *24* (4), 265-281.
13. Screnci, D.; McKeage, M. J., Platinum neurotoxicity: clinical profiles, experimental models and neuroprotective approaches. *J. Inorg. Biochem.* **1999**, *77* (1), 105-110.
14. Galluzzi, L.; Senovilla, L.; Vitale, I.; Michels, J.; Martins, I.; Kepp, O.; Castedo, M.; Kroemer, G., Molecular mechanisms of cisplatin resistance. *Oncogene* **2011**, *31* (15), 1869-1883.
15. Shen, D.-W.; Pouliot, L. M.; Hall, M. D.; Gottesman, M. M., Cisplatin resistance: a cellular self-defense mechanism resulting from multiple epigenetic and genetic changes. *Pharmacol. Rev.* **2012**, *64* (3), 706-721.
16. Thun, M. J.; Henley, S. J.; Patrono, C., Nonsteroidal anti-inflammatory drugs as anticancer agents: mechanistic, pharmacologic, and clinical issues. *J. Natl. Cancer I.* **2002**, *94* (4), 252-266.
17. Tosco, P.; Lazzarato, L., Mechanistic insights into cyclooxygenase irreversible inactivation by aspirin. *ChemMedChem* **2009**, *4* (6), 939-945.
18. Vane, J. R., Inhibition of prostaglandin synthesis as a mechanism of action for aspirin-like drugs. *Nature* **1971**, *231* (25), 232-235.

19. Mukherjea, D.; Rybak, L. P.; Sheehan, K. E.; Kaur, T.; Ramkumar, V.; Jajoo, S.; Sheth, S., The design and screening of drugs to prevent acquired sensorineural hearing loss. *Expert Opin. Drug Dis.* **2011**, *6* (5), 491-505.
20. Grilli, M.; Pizzi, M.; Memo, M.; Spano, P., Neuroprotection by aspirin and sodium salicylate through blockade of NF- κ B activation. *Science* **1996**, *274* (5291), 1383-1385.
21. Oeth, P.; Mackman, N., Salicylates inhibit lipopolysaccharide-induced transcriptional activation of the tissue factor gene in human monocytic cells. *Blood* **1995**, *86* (11), 4144-4152.
22. Yin, M.-J.; Yamamoto, Y.; Gaynor, R. B., The anti-inflammatory agents aspirin and salicylate inhibit the activity of I κ B kinase- β . *Nature* **1998**, *396* (6706), 77-80.
23. Bharti, A. C.; Donato, N.; Singh, S.; Aggarwal, B. B., Curcumin (diferuloylmethane) down-regulates the constitutive activation of nuclear factor- κ B and I κ B α kinase in human multiple myeloma cells, leading to suppression of proliferation and induction of apoptosis. *Blood* **2003**, *101* (3), 1053-1062.
24. Singh, S.; Aggarwal, B. B., Activation of transcription factor NF- κ B is suppressed by curcumin (diferuloylmethane). *J. Biol. Chem.* **1995**, *270* (42), 24995-25000.
25. Pu, H.-L.; Chiang, W.-L.; Maiti, B.; Liao, Z.-X.; Ho, Y.-C.; Shim, M. S.; Chuang, E.-Y.; Xia, Y.; Sung, H.-W., Nanoparticles with Dual Responses to Oxidative Stress and Reduced pH for Drug Release and Anti-inflammatory Applications. *ACS Nano* **2014**, *8* (2), 1213-1221.
26. Anand, P.; Kunnumakkara, A. B.; Newman, R. A.; Aggarwal, B. B., Bioavailability of curcumin: problems and promises. *Mol. Pharm.* **2007**, *4* (6), 807-818.

27. Davis, S.; Weiss, M.; Wong, J.; Lampidis, T. J.; Chen, L. B., Mitochondrial and plasma membrane potentials cause unusual accumulation and retention of rhodamine 123 by human breast adenocarcinoma-derived MCF-7 cells. *J. Biol. Chem.* **1985**, *260* (25), 13844-13850.
28. Marrache, S.; Dhar, S., Engineering of blended nanoparticle platform for delivery of mitochondria-acting therapeutics. *Proc. Natl. Acad. Sci.* **2012**, *109* (40), 16288-16293.
29. Mehar, A.; Macanas-Pirard, P.; Mizokami, A.; Takahashi, Y.; Kass, G. E.; Coley, H. M., The effects of cyclooxygenase-2 expression in prostate cancer cells: modulation of response to cytotoxic agents. *J. Pharmacol. Exp. Ther.* **2008**, *324* (3), 1181-7.
30. Mitchell, J. A.; Akarasereenont, P.; Thiemermann, C.; Flower, R. J.; Vane, J. R., Selectivity of nonsteroidal antiinflammatory drugs as inhibitors of constitutive and inducible cyclooxygenase. *Proc. Natl. Acad. Sci. USA* **1993**, *90* (24), 11693-7.
31. Graf, N.; Lippard, S. J., Redox activation of metal-based prodrugs as a strategy for drug delivery. *Adv. Drug Delivery Rev.* **2012**, *64* (11), 993-1004.
32. Sato, Y.; Goto, Y.; Narita, N.; Hoon, D. S., Cancer Cells Expressing Toll-like Receptors and the Tumor Microenvironment. *Cancer Microenviron.* **2009**, *2 Suppl 1*, 205-14.
33. Marrache, S.; Tundup, S.; Harn, D. A.; Dhar, S., Ex vivo programming of dendritic cells by mitochondria-targeted nanoparticles to produce interferon-gamma for cancer immunotherapy. *ACS Nano* **2013**, *7* (8), 7392-402.

CHAPTER 4

CONCLUSION AND OUTLOOK

Conclusions

This thesis has introduced and described a different approach toward combination therapy as a way to treat cancer with nanotechnology. Chapter 1 is a literature review on combination therapy; it introduces the advantages of combination therapy over conventional therapy. Nanotechnology used in medicine and its properties were explored to describe different delivery vehicles specifically biodegradable polymeric NPs. Furthermore, surface modification of delivery vehicles to overcome biological barriers was discussed.

Chapter 2 describes a combination of photodynamic therapy and immunotherapy. ZnPc, a photosensitizer, was encapsulated noncovalently in the NPs with CpG-ODN, an immunoadjuvant, on the surface of NPs. Irradiation of ZnPc induced ROS to eradicate cancer cells and CpG-ODN activated DCs that communicate with cancer-specific antigens from cancer cells eradicated by ZnPc to stimulate the immune system. ZnPc and CpG-ODN in a single NP platform provided better phototoxicity and immune response than combining them in a free form.

Chapter 3 demonstrates chemo-anti-inflammatory therapy. Platin-A, a prodrug developed by Dr. Rakesh Pathak in our lab from aspirin, a common anti-inflammatory drug and a chemotherapeutic cisplatin can cause cancer cell deaths and lower inflammation simultaneously. The cytotoxicity of Platin-A is comparable to that of a mixture of cisplatin and aspirin together. Also, it represents an anti-inflammatory property by lowering the levels of

COX-2. Curcumin, an anti-inflammatory compound, was conjugated with cisplatin in a prodrug form, Platin-C.

Future Work

This thesis has addressed different combination therapy methods to synergistically increase the efficacy of treating cancer through the use of nanotechnology.

Further work on testing the different properties of Platin-C needs to be performed.

Photoimmunotherapy with ZnPc NPs with immunostimulant has shown potential to increase the immune response. The next step of this project would be to maximize the immune response by optimizing the system such as concentration or ratio between cisplatin and curcumin and furthermore, it would be tested in animal model.

Final Remarks

As combination therapy becomes an efficient strategy in the control of cancer, finding different method of combination therapy with biodegradable polymeric NPs will provide efficacious aids for cancer treatment. This thesis is a fundamental study in developing a method to remedy a deficiency in conventional therapy. The ability to target multiple actions can lead to improving current therapy practices. Moreover, easily modified polymeric NPs can create a method to ensure accumulation of drugs in more specific targets. Together, it can improve the performance on treating cancer efficiently.